A TRANSMISSION METHOD FOR DETERMINING THE OPTICAL CONSTANTS OF METALS

by

Per Joensen

B.Sc., Simon Fraser University, 1970

A THESIS SUBMITTED IN PARTIAL FULFILMENT OF

THE REQUIREMENTS FOR THE DEGREE OF

MASTER OF SCIENCE

in the Department

of

Physics

SIMON FRASER UNIVERSITY

February 1973

APPROVAL

Name: Per Joen Joensen

Degree: Master of Science

Title of Thesis: A Transmission Method for Determining the Optical Constants of Metals

Examining Committee: Date Approved: Feb 11, 1972

Chairman: K.E. Rieckhoff

J.C. Irwin
Senior Supervisor

J.F. Cochran

A.E. Curzon

B.P. Clayman

PARTIAL COPYRIGHT LICENSE

I hereby grant to Simon Fraser University the right to lend my thesis or dissertation (the title of which is shown below) to users of the Simon Fraser University Library, and to make partial or single copies only for such users or in response to a request from the library of any other university, or other educational institution, on its own behalf or for one of its users. I further agree that permission for multiple copying of this thesis for scholarly purposes may be granted by me or the Dean of Graduate Studies. It is understood that copying or publication of this thesis for financial gain shall not be allowed without my written permission.

Title of Thesis/Dissertation:

"A Transmission Method for Determinining the Optical Constants of Metals"

Author:

(signature)

Per Joensen

(name)

March 5, 1973

(date)

ABSTRACT

A technique is described for determining the optical constants of an arbitrary material by shining monochromatic light through thin films of the material and measuring the transmissivity and the phase change on transmission for samples of various thicknesses. The results are characteristic of the bulk material and are insensitive to surface effects. The technique was tested at wavelengths of 4880Å, 5145Å, and 6328Å on vacuum-deposited gold films with thicknesses in the range 170Å to 1800Å. The results obtained for the optical constants of gold are, within the experimental error of our technique, in agreement with other authors' values obtained from reflection measurements.

TABLE OF CONTENTS

LIST OF TABLES

LIST OF FIGURES

ACKNOWLEDGEMENTS

Special thanks are due Dr. A.E. Curzon, who prepared the samples and measured their thicknesses. I am also indebted to Dr. J.C. Irwin, who supervised and encouraged the research reported in this thesis, and to Dr. J.F. Cochran, who suggested the experiment and participated in helpful discussions.

CHAPTER 1

INTRODUCTION

The optical constants of metals have, for many years, been measured using techniques involving reflection measurements. The results obtained using these methods are sensitive to surface properties. It is therefore desirable to employ a technique which utilizes only transmission measurements, because the values of the optical constants obtained from transmission measurements are not sensitive to surface effects and thus should be truly representative of the bulk values.

A brief survey of common techniques for measuring optical constants of metals will first be presented. Although the techniques to be described are applicable to homogeneous solids in general, they are especially suitable for materials with high reflectivities and large absorption coefficients. Accordingly, these techniques are usually associated with metals.

Consider a thin metallic film of thickness d and refractive index $\hat{n} = n-ik$ mounted on a non-absorbing substrate. Let the reflectivity (the ratio of reflected to incident intensities) for light incident from the metal side be designated R, and let the reflectivity for light incident from the substrate side be R^1. The transmissivity (the ratio of transmitted to incident intensities) is designated T, and is the same in both directions.

From measurements of R, R^1, and T at normal or oblique incidence, it is possible, utilizing appropriate theoretical

expressions, to determine the optical constants n and k, and the thickness d (Abelès, 1971, p. 182). These quantities can also be determined from oblique-incidence measurements of R and T alone (Nestell and Christy, 1972). n and k can also be determined from measured values of R, T, and d (Abelès, 1971, p. 187; Thèye, 1970, p. 3062), where the measurement of the thickness d can be accomplished by any of numerous possible methods (Heavens, 1965, Chapter 5); three of the most commonly used methods are described in section 3-3.

If it is desired to avoid measuring T, and to work with a bulk sample, using only one surface, n and k can be determined from the Kramers-Kronig relations using measurements of R only (Abelès, 1971, p. 183). However, the calculation requires that R be known at all frequencies from zero to infinity. In practice, R is measured in a finite frequency range and assumptions are made concerning the variation of R with frequency outside the measured range. The accuracy of the results thus not only depends critically on the surface conditions but also on how well these assumptions approximate reality.

Ellipsometric methods (Abelès, 1971, p. 185; Heavens, 1964, p. 218; Givens, 1958, p. 336) for determining the optical constants of a metal involve shining a beam of plane-polarized light onto the surface of a bulk sample, at a measured angle of incidence, and analyzing the elliptically polarized reflected beam. Light polarized parallel to the plane of incidence interacts with the surface of the metal in a different manner than

light with the orthogonal polarization, since the electrons in the metal are accelerated parallel to the surface in the latter case, while in the former case there is a component of the electric field perpendicular to the surface. The phase difference between the components having the electric vector parallel and perpendicular to the plane of incidence is measured, and the ratio of the amplitudes of the two components is also measured. Assuming that n and k are the same for both polarizations, n and k can then be calculated; the appropriate equations have been written down by Givens (1958, p. 337).

In addition to the aforementioned methods, many combinations and variations of these techniques have been used (Hunderi, 1972; Abelès, 1971, p. 187; Heavens, 1965, p. 133; Heavens, 1964, p. 229).

In summary, optical constants of metals are commonly measured by means of techniques that involve shining light on a sample and measuring, either solely or in combination with other measurements, the reflectivity and/or the phase change on reflection from the surface of the material. These techniques employ surface measurements to determine bulk properties; such techniques are extremely sensitive to surface contamination and other surface anomalies (Heavens, 1965, p. 131), and the results for the bulk parameters can be wildly in error.

The technique that will be described in this thesis involves the measurement of the transmissivity and the phase change on transmission for light passing through various

samples of known thickness. n is determined from a measurement of the change in phase shift with thickness, and k is determined from the measured thickness dependence of the transmissivity. This method has the advantage that the light traverses a bulk specimen; there is no doubt that the bulk properties are indeed being measured. In contrast to reflection methods, our transmission method is insensitive to surface properties, and is therefore not as critically dependent on the conditions of preparation and storage of samples.

Other authors have used transmission techniques to determine the optical constants of non-metals (Brattain and Briggs, 1949; Haysman and Lenham, 1972). However, the transmission experiments performed previously on highly-absorbing materials have involved measuring only the transmissivity; these experiments allow the determination of k only. Schulz (1957, p. 121) has determined k for silver in the infra-red and visible by studying transmissivity versus thickness, using silver films up to 800Å thick.

Although transmission methods have been used before, the phase changes on transmission through films which absorb very strongly over distances of less than one wavelength have not, to the author's knowledge, been measured previous to this work.

The theoretical description of light passing through a thin film is outlined in Chapter 2 of this thesis; theoretical expressions for the transmissivity and the phase change on transmission are derived as functions of the optical constants of the film, and simplified expressions pertaining to the thick-film limit are presented. Our technique involves measuring transmissivities and phase changes for films of various thicknesses, and using the thickness dependences of these measurements, in the thick-film limit, to determine the optical constants of the material. The method of making the experimental measurements is described in Chapter 3, and our procedure for determining the optical constants from these measurements is presented, with our experimental results, in Chapter 4. Chapter 5 contains an evaluation of the technique and suggestions for further work.

CHAPTER 2

OPTICAL PROPERTIES OF THIN METALLIC FILMS

2-1 Propagation of Electromagnetic Radiation in Conducting Media

The propagation of electromagnetic radiation in an unbounded isotropic conducting medium will first be considered. The electric and magnetic fields are determined by Maxwell's equations:

$$\text{curl } \vec{E} = -\frac{1}{c}\frac{\partial \vec{B}}{\partial t} \tag{1}$$

$$\text{curl } \vec{H} = \frac{1}{c}\frac{\partial \vec{D}}{\partial t} + \frac{4\pi}{c}\vec{J} \tag{2}$$

$$\text{div } \vec{D} = 4\pi\rho \tag{3}$$

$$\text{div } \vec{B} = 0 \tag{4}$$

in Gaussian units, where $\vec{B} = \mu\vec{H}$, $\vec{D} = \varepsilon E$, and $\vec{J} = \sigma\vec{E}$; the symbols have their usual meanings (Purcell, 1965; Jackson, 1962; Born and Wolf, 1965, p. 611; Garbuny, 1965, p. 248). In a metal, at optical frequencies, we can set $\text{div } \vec{D} = 0$ because any charges induced by the fields are neutralized in a relaxation time which is very much less than the period of oscillation of the wave (Born and Wolf, 1965, p. 612).

Equations (1) and (2) can be written in the form

$$\text{curl } \vec{E} = -\frac{\mu}{c}\frac{\partial \vec{H}}{\partial t} \tag{1'}$$

$$\text{curl } \vec{H} = \frac{\varepsilon}{c} \frac{\partial \vec{E}}{\partial t} + \frac{4\pi\sigma \vec{E}}{c} \quad . \tag{2'}$$

Let $\vec{E}$ and $\vec{H}$ be oriented respectively along x and y in a right-handed co-ordinate system. Then (1') and (2') reduce to

$$\frac{\partial E}{\partial z} = - \frac{\mu}{c} \frac{\partial H}{\partial t} \tag{3}$$

and

$$- \frac{\partial H}{\partial z} = \frac{\varepsilon}{c} \frac{\partial E}{\partial t} + \frac{4\pi\sigma E}{c} \quad . \tag{4}$$

Assuming a monochromatic field with time dependences of the form $E = E_o e^{\pm i\omega t}$ and $H = H_o e^{\pm i\omega t}$, we have $\frac{\partial E}{\partial t} = i\omega E$ and $\frac{\partial H}{\partial t} = i\omega H$. From equations (3) and (4) we obtain:

$$\frac{\partial E}{\partial z} = - \frac{\mu}{c} i\omega H \tag{5}$$

and

$$- \frac{\partial H}{\partial z} = \frac{\varepsilon}{c} i\omega E + \frac{4\pi\sigma}{c} E \quad . \tag{6}$$

Differentiating equation (5) with respect to z, we have

$$\frac{\partial^2 E}{\partial z^2} = - \frac{\mu}{c} i\omega \frac{\partial H}{\partial z} \quad . \tag{7}$$

Equations (6) and (7) yield:

$$- \frac{\mu}{c} i\omega \frac{\partial H}{\partial z} = \frac{\mu}{c} i\omega \left(\frac{\varepsilon}{c} i\omega E \right) + \frac{\mu}{c} i\omega \left(\frac{4\pi\sigma}{c} E \right)$$

$$= \frac{\partial^2 E}{\partial z^2}$$

or $$\frac{\partial^2 E}{\partial z^2} = \left[- \left(\frac{\omega}{c} \right)^2 \varepsilon\mu + i\omega \frac{4\pi\mu\sigma}{c^2} \right] E \quad . \tag{8}$$

Assuming spatial variation of the form $E = E_o e^{-ikz}$, we have

$$\frac{\partial^2 E}{\partial z^2} = -k^2 E.$$

Thus

$$k^2 = \left(\frac{\omega}{c}\right)^2 \varepsilon\mu - i\omega \frac{4\pi\mu\sigma}{c^2}$$

$$= \left(\frac{\omega}{c}\right)^2 \mu\left[\varepsilon - i \frac{4\pi\sigma}{\omega}\right] \tag{9}$$

or $$k^2 = \left(\frac{\omega}{c}\right)^2 \mu\hat{\varepsilon} = k_o^2 \mu\hat{\varepsilon} \tag{10}$$

where $\hat{\varepsilon}$ is the complex dielectric constant of the material. $\hat{\varepsilon}$ can be written

$$\hat{\varepsilon} = \varepsilon_1 - i\varepsilon_2 . \tag{11}$$

The components of $\hat{\varepsilon}$ satisfy

$$\varepsilon_1 = \varepsilon \tag{12}$$

and

$$\varepsilon_2 = \frac{4\pi\sigma}{\omega} . \tag{13}$$

We now define a complex refractive index

$$\hat{n} = n - ik = \sqrt{\mu\hat{\varepsilon}} , \tag{14}$$

where n and k are real and non-negative. We can set $\mu = 1$, since this is a good approximation for all materials at optical frequencies. Thus $\hat{\varepsilon} = \hat{n}^2$, and

$$\varepsilon_1 = n^2 - k^2 \tag{15}$$

$$\varepsilon_2 = 2nk . \tag{16}$$

the wave can be written

$$E = E_o e^{+i\omega t} e^{-ikz}$$

$$= E_o \exp\left\{i\left(\omega t - \frac{2\pi\hat{n}z}{\lambda_o}\right)\right\} \qquad (17)$$

since $k = k_o\hat{n} = \frac{\omega}{c}\hat{n} = \frac{2\pi\hat{n}}{\lambda_o}$, where λ_o is the wavelength of light outside the material. Equation (17), representing a wave propagating in the positive z-direction, requires that $\hat{n}$ be written $\hat{n} = n - ik$ so that, for positive k, the amplitude of the wave decreases as z increases.

The main point we wish to make here is that the optical properties of a material can be specified by assigning to the material a complex refractive index $\hat{n} = n - ik$. n and k are called the optical "constants" of the material, even though they vary strongly with frequency.

n, the real part of the refractive index of the material, satisfies the relation

$$n = \frac{\lambda_o}{\lambda_i} \quad , \qquad (18)$$

where λ_i is the wavelength of light inside the material. This is the same relation satisfied by a transparent medium of (real) refractive index n. However, in the general case of non-normal incidence, the relationship between the angle of incidence and the angle of refraction (Heavens, 1965, p. 49) is more complicated than Snell's law.

The amplitude of the wave inside the material decreases by a factor $e^{2\pi k}$ over a distance λ_o, which is one wavelength outside the material. k is usually called the extinction coefficient of the material. The intensity of the wave inside the material decreases by a factor $e^{4\pi k}$ over a distance λ_o. If I_1 and I_2 are the intensities at distances z_1 and z_2 inside the material, we can write

$$I_2 = I_1 e^{-\alpha(z_2 - z_1)}, \tag{19}$$

where α, called the absorption coefficient, is related to the extinction coefficient k by

$$\alpha = \frac{4\pi k}{\lambda_o} . \tag{20}$$

Our exposition has so far ignored the presence of boundaries between media. In the next section, we will apply boundary conditions to deal with the special case of transmission of light through thin metallic films.

2-2 Transmission of Electromagnetic Radiation Through Thin Films

The problem we wish to consider is the following: what is the transmissivity (fraction of incident intensity transmitted) and what is the phase change on transmission for normally-incident monochromatic light of wavelength λ_o passing from a non-absorbing medium of refractive index n_o, through a plane-parallel absorbing film of thickness d and complex refractive index $\hat{n} = n - ik$, into a non-absorbing medium of refractive index n_s?

As indicated in Figure 1, we represent the amplitude of the incident electric field by E_o^+, and the amplitude of the reflected wave by E_o^-. Inside the film, E_1^+ and E_1^- correspond to the vector sum of all waves travelling to the right and to the left, respectively. E_2^+ is the amplitude of the transmitted wave in the medium of index n_s. The incident wave is travelling in the positive z-direction, and is incident normally on the film. $\vec{E}$ is polarized along x, and $\vec{H}$ along y. Let the first boundary be defined by the plane $z = 0$; the second boundary is at $z = d$.

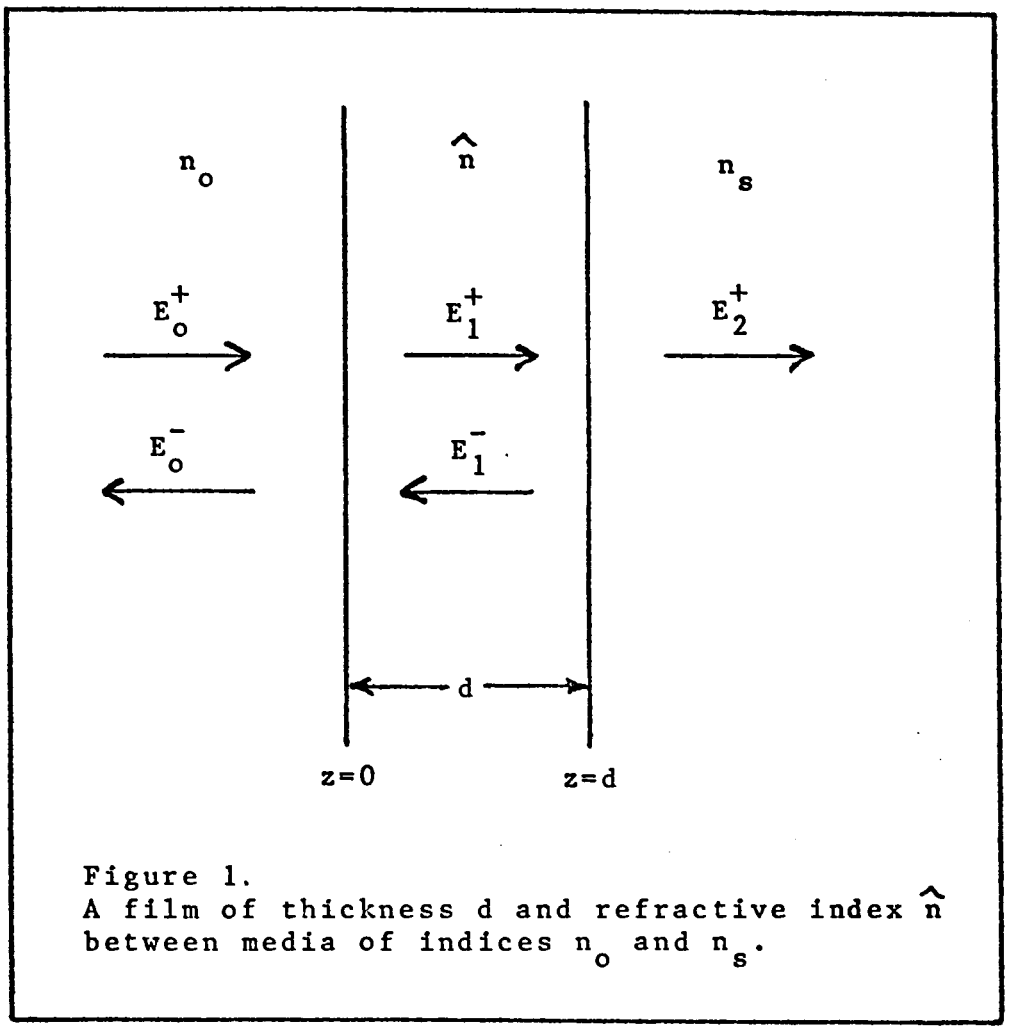

Figure 1.
A film of thickness d and refractive index $\hat{n}$ between media of indices n_o and n_s.

Let

$$\frac{2\pi n_o}{\lambda_o} = q_o \quad , \tag{21}$$

$$\frac{2\pi \hat{n}}{\lambda_o} = q_1 \quad , \tag{22}$$

and

$$\frac{2\pi n_s}{\lambda_o} = q_2 \quad . \tag{23}$$

The z-dependent parts of the electric field $\vec{E}$ and the magnetic field $\vec{H}$ (where we have assumed $\mu = 1$) in the three different regions are given by (Heavens, 1965, p. 60):

$$E_o = E_o^+ e^{-iq_o z} + E_o^- e^{+iq_o z} \tag{24}$$

$$H_o = n_o(E_o^+ e^{-iq_o z} - E_o^- e^{+iq_o z}) \tag{25}$$

$$E_1 = E_1^+ e^{-iq_1 z} + E_1^- e^{+iq_1 z} \tag{26}$$

$$H_1 = \hat{n}(E_1^+ e^{-iq_1 z} - E_1^- e^{+iq_1 z}) \tag{27}$$

$$E_2 = E_2^+ e^{-iq_2 z} \tag{28}$$

$$H_2 = n_s E_2^+ e^{-iq_2 z} \quad . \tag{29}$$

The tangential components of $\vec{E}$ and $\vec{H}$ are continuous across the boundaries. Applying these conditions, we have:

$$E_o = E_1 \text{ at } z = 0 \Rightarrow E_o^+ + E_o^- = E_1^+ + E_1^- \tag{30}$$

$$H_o = H_1 \text{ at } z = 0 \Rightarrow n_o(E_o^+ - E_o^-) = \hat{n}(E_1^+ - E_1^-) \tag{31}$$

$$E_1 = E_2 \text{ at } z = d \Rightarrow E_1^+ e^{-iq_1 d} + E_1^- e^{+iq_1 d} = E_2^+ \tag{32}$$

$$H_1 = H_2 \text{ at } z = d \Rightarrow \hat{n}(E_1^+ e^{-iq_1 d} - E_1^- e^{+iq_1 d}) = n_s E_2^+ \quad . \tag{33}$$

Solving equations (30) and (31) for E_o^+ and E_o^-, we obtain

$$E_o^+ = \frac{n_o+\hat{n}}{2n_o} E_1^+ + \frac{n_o-\hat{n}}{2n_o} E_1^- \tag{34}$$

and

$$E_o^- = \frac{n_o-\hat{n}}{2n_o} E_1^+ + \frac{n_o+\hat{n}}{2n_o} E_1^- \quad . \tag{35}$$

Solving equations (32) and (33) for $E_1^+ e^{-iq_1 d}$ and $E_1^- e^{+iq_1 d}$,

$$E_1^+ e^{-iq_1 d} = \frac{\hat{n}+n_s}{2\hat{n}} E_2^+ \tag{36}$$

$$E_1^- e^{+iq_1 d} = \frac{\hat{n}-n_s}{2\hat{n}} E_2^+ \quad . \tag{37}$$

At the first and second boundaries, respectively, the amplitude reflection coefficients are

$$r_1 = \frac{n_o-\hat{n}}{n_o+\hat{n}} = \frac{n_o-n+ik}{n_o+n-ik} \tag{38}$$

and

$$r_2 = \frac{\hat{n}-n_s}{\hat{n}+n_s} = \frac{n-ik-n_s}{n-ik+n_s} \quad . \tag{39}$$

The amplitude transmission coefficients at the first and second interfaces, respectively, are

$$t_1 = \frac{2n_o}{n_o+\hat{n}} = \frac{2n_o}{n_o+n-ik} \tag{40}$$

and

$$t_2 = \frac{2\hat{n}}{\hat{n}+n_s} = \frac{2(n-ik)}{n-ik+n_s} \quad . \tag{41}$$

In terms of these coefficients, equations (34) to (37) can be written

$$E_o^+ = \frac{1}{t_1} E_1^+ + \frac{r_1}{t_1} E_1^- \tag{42}$$

$$E_o^- = \frac{r_1}{t_1} E_1^+ + \frac{1}{t_1} E_1^- \tag{43}$$

$$E_1^+ e^{-iq_1 d} = \frac{1}{t_2} E_2^+ \tag{44}$$

$$E_1^- e^{+iq_1 d} = \frac{r_2}{t_2} E_2^+ \quad . \tag{45}$$

The amplitude reflection coefficient for the film is thus

$$r = \frac{E_o^-}{E_o^+} = \frac{r_1 + \left(\frac{E_1^-}{E_1^+}\right)}{1 + r_1 \left(\frac{E_1^-}{E_1^+}\right)} \tag{46}$$

and the amplitude transmission coefficient for the film is

$$t = \frac{E_2^+}{E_o^+} = \frac{t_1 t_2 \, e^{-iq_1 d}}{1 + r_1 \left(\frac{E_1^-}{E_1^+}\right)} \quad . \tag{47}$$

From equations (44) and (45),

$$\frac{E_1^-}{E_1^+} = r_2 e^{-2iq_1 d} \quad , \tag{48}$$

so equations (46) and (47) can be written

$$r = \frac{r_1 + r_2 \, e^{-2i\delta}}{1 + r_1 r_2 \, e^{-2i\delta}} \tag{49}$$

and

$$t = \frac{t_1 t_2 \, e^{-i\delta}}{1 + r_1 r_2 \, e^{-2i\delta}} \quad , \tag{50}$$

where $\delta = q_1 d = \frac{2\pi}{\lambda_o} \hat{n} d = \frac{2\pi}{\lambda_o} (n - ik) d.$ (51)

From equation (51),

$$e^{\pm i\delta} = \exp\left(\pm \frac{2\pi kd}{\lambda_o}\right) \exp\left(\pm i \frac{2\pi nd}{\lambda_o}\right)$$

$$= e^{\pm K}(\cos N \pm i \sin N) \qquad (52)$$

where $K = \frac{2\pi kd}{\lambda_o}$ and $N = \frac{2\pi nd}{\lambda_o}$. N is the phase change in traversing the film, excluding the phase changes at the surfaces.

Equation (49) can be written in the form

$$r = \frac{r_1 e^{i\delta} + r_2 e^{-i\delta}}{e^{i\delta} + r_1 r_2 e^{-i\delta}}$$

$$= \frac{(n_o-\hat{n})(\hat{n}+n_s)e^{i\delta} + (n_o+\hat{n})(\hat{n}-n_s)e^{-i\delta}}{(n_o+\hat{n})(\hat{n}+n_s)e^{i\delta} + (n_o-\hat{n})(\hat{n}-n_s)e^{-i\delta}}, \qquad (53)$$

where we have substituted r_1 and r_2 from equations (38) and (39).

Equation (53) can be written in the form

$$r = \frac{A+iB}{C+iD}. \qquad (54)$$

Solving for A, B, C, and D, we obtain:

$$A = [(n_o-n)(n+n_s)+k^2]e^{K}\cos N + k(n_o-2n-n_s)e^{K}\sin N$$

$$+ [(n_o+n)(n-n_s)-k^2]e^{-K}\cos N - k(n_o+2n-n_s)e^{-K}\sin N, \quad (55)$$

$$B = [(n_o-n)(n+n_s)+k^2]e^{K}\sin N - k(n_o-2n-n_s)e^{K}\cos N$$

$$- [(n_o+n)(n-n_s)-k^2]e^{-K}\sin N + k(n_o+2n-n_s)e^{-K}\cos N, \quad (56)$$

$$C = [(n_o+n)(n+n_s)-k^2]e^{K}\cos N + k(n_o+2n+n_s)e^{K}\sin N$$

$$+ [(n_o-n)(n-n_s)+k^2]e^{-K}\cos N - k(n_o-2n+n_s)e^{-K}\sin N \quad (57)$$

$$D = [(n_o+n)(n+n_s)-k^2]e^{K}\sin N - k(n_o+2n+n_s)e^{K}\cos N$$

$$- [(n_o-n)(n-n_s)+k^2]e^{-K}\sin N + k(n_o-2n+n_s)e^{-K}\cos N . \quad (58)$$

Separating the amplitude reflection coefficient into its real and imaginary parts, we have, from equation (54):

$$r = \frac{A+iB}{C+iD} = \frac{AC+BD}{C^2+D^2} + i \cdot \frac{BC-AD}{C^2+D^2} . \quad (59)$$

The reflectivity of the film is

$$R = |r|^2 = rr^* = \frac{A^2+B^2}{C^2+D^2} . \quad (60)$$

The phase change on reflection is

$$\Delta = \arctan\left(\frac{BC-AD}{AC+BD}\right). \quad (61)$$

Next, we will calculate the transmissivity of the film

and the phase change on transmission. Equation (50) can be written in the form

$$t = \frac{t_1 t_2}{e^{i\delta} + r_1 r_2 \, e^{-i\delta}}$$

$$= \frac{4 n_o \hat{n}}{(n_o+\hat{n})(\hat{n}+n_s)e^{i\delta} + (n_o-\hat{n})(\hat{n}-n_s)e^{-i\delta}} \qquad (62)$$

where we have again substituted r_1 and r_2 from equations (38) and (39). The denominator on the right-hand side of equation (62) is the same as the denominator in equation (53). The amplitude transmission coefficient can thus be written

$$t = \frac{4 n_o (n-ik)}{C+iD} \quad . \qquad (63)$$

The transmissivity of the film is

$$T = \frac{n_s}{n_o} |t|^2 = \frac{n_s}{n_o} tt^*$$

$$= \frac{16 \, n_o n_s (n^2+k^2)}{C^2+D^2} \quad . \qquad (64)$$

Separating the amplitude transmission coefficient into its real and imaginary parts, we have, from equation (63):

$$t = \frac{4 \, n_o (nC-kD)}{C^2+D^2} - i \cdot \frac{4 \, n_o (nD+kC)}{C^2+D^2} \quad . \qquad (65)$$

The phase change on transmission is thus

$$\gamma = \arctan\left(\frac{nD+kC}{kD-nC}\right) \quad . \qquad (66)$$

We have now established the desired formulae. Equations

(64) and (66), with C and D substituted from equations (57) and (58), give the transmissivity and the phase change on transmission in terms of n, k, n_o, n_s, λ_o, and d.

The derivation presented here has followed that of O.S. Heavens (1965, pp. 59-62 and pp. 89-92). In passing, a few misprints that exist in Heavens' book should be noted:

(a) the lower of equations 4(68) on page 61 should be in the form of our equation (45), with the phase factor e^{-iq_2d} left in, although we have chosen to omit it;

(b) equation 4(130) on page 90 should read

$$R_o = \frac{r_1 + r_1r_2^2 + (r_2+r_1^2r_2)\cos 2\delta_1}{1 + 2r_1r_2\cos 2\delta_1 + r_1^2r_2^2} - i \cdot \frac{(r_2-r_1^2r_2)\sin 2\delta_1}{1 + 2r_1r_2\cos 2\delta_1 + r_1^2r_2^2};$$

(c) equation 4(132) on page 90 should read

$$\tan \Delta_o = \frac{-r_2(1-r_1^2)\sin 2\delta_1}{r_1(1+r_2^2) + r_2(1+r_1^2)\cos 2\delta_1} ;$$

(d) equation 4(140) on page 91 should be in the form of our equation (61).

Born and Wolf (1965, pp. 627-630) have presented a similar derivation, but their expressions for the transmissivity and the phase change on transmission appear to be incorrect. Curves of transmissivity versus film thickness

and phase change versus film thickness, plotted using Born and Wolf's expressions, do not exhibit the correct limiting behaviour for small thicknesses.

If one wishes to compare the results of experimental measurements of the transmissivity or the phase change on transmission with theory, one must remember that equations (64) and (66) apply to the configuration drawn in Figure 1, where only two interfaces are considered. In practice, this is sufficient if $n_o = n_s = 1$, as is the case for a film suspended over an aperture. For a film mounted on a substrate, however, measurements are not performed inside the substrate; the back surface of the substrate is an additional interface that must be taken into account. This can be done theoretically (Heavens, 1965, pp. 62-63), but in our case the effect of the substrate on the measured quantity of interest (the transmissivity) was made negligible. It should be noted that our phase shift measurements were performed on suspended films, and transmissivity measurements were performed on films on substrates. The reasons for carrying out the measurements in this manner will be given at the end of section 3-5-4.

2-3 The Thick-film Limit

We will now derive a simplified expression for the amplitude transmission coefficient in the thick-film limit where the product kd is sufficiently large that

$$e^{-\frac{4\pi kd}{\lambda_o}} << 1 \quad .$$

Going back to equations (30) to (33), we have, for the case $n_o = n_s = 1$:

$$E_o^+ + E_o^- = E_1^+ + E_1^- \tag{30}$$

$$E_o^+ - E_o^- = \hat{n}(E_1^+ - E_1^-) \tag{31^1}$$

$$E_2^+ = E_1^+ e^{-iq_1 d} + E_1^- e^{iq_1 d} \tag{32}$$

$$E_2^+ = \hat{n}(E_1^+ e^{-iq_1 d} - E_1^- e^{iq_1 d}) \quad . \tag{33^1}$$

In a thick film, E_1^- is very small compared to E_1^+. We then have, approximately, a decoupling between the front and back surfaces. At the front surface ($z = 0$),

$$E_o^+ + E_o^- = E_1^+ \tag{67}$$

and

$$E_o^+ - E_o^- = \hat{n}E_1^+ \quad . \tag{68}$$

Adding (67) and (68), we obtain

$$2E_o^+ = (1 + \hat{n})E_1^+ \quad .$$

or

$$\frac{E_1^+}{E_o^+} = \frac{2}{(1+\hat{n})} \quad . \tag{69}$$

At the back surface (z = d),

$$E_1^+ \, e^{-iq_1 d} + E_1^- \, e^{iq_1 d} = \hat{n} E_1^+ \, e^{-iq_1 d} - \hat{n} E_1^- \, e^{iq_1 d} \quad , \tag{70}$$

from which it follows that

$$\frac{E_1^-}{E_1^+} = \left(\frac{\hat{n}-1}{\hat{n}+1}\right) e^{-2iq_1 d} . \tag{71}$$

Thus

$$t = \frac{E_2^+}{E_o^+} = \frac{4\hat{n}}{(1+\hat{n})^2} \, e^{-iq_1 d}$$

$$= \frac{4\hat{n}}{(1+\hat{n})^2} \, e^{-i\left(\frac{2\pi\hat{n}d}{\lambda_o}\right)}$$

$$= \frac{4\hat{n}}{(1+\hat{n})^2} \, e^{-\frac{2\pi i n d}{\lambda_o}} \cdot e^{-\frac{2\pi k d}{\lambda_o}} \quad . \tag{72}$$

The optical constants n and k can thus be determined by measuring the change of transmitted amplitude (or intensity) with thickness to obtain $\frac{2\pi k}{\lambda_o}$ (or $\frac{4\pi k}{\lambda_o}$), and the change of phase with thickness to obtain $\frac{2\pi n}{\lambda_o}$, using films which are sufficiently thick that multiple reflections inside the films may be neglected.

CHAPTER 3

DESCRIPTION OF THE EXPERIMENT

3-1 Introduction

The experiment consisted of measuring the transmissivity and the phase change on transmission for monochromatic visible light passing through gold films of various thicknesses. The measurements were conducted at normal incidence and at atmospheric pressure and room temperature. The optical constants n and k (the real and imaginary parts of the complex refractive index $\hat{n} = n-ik$) were then determined from these measurements. The technique can be used on films of an arbitrary material, but is especially suitable for thin films of a strongly-absorbing material. Gold was chosen for this study because of its stability against oxidation, and because the optical constants of gold change considerably with wavelength in the range 4880Å to 6328Å, which is the regime in which it was found convenient to work. Argon laser lines at 4880Å and 5145Å, and the helium-neon laser line at 6328Å were chosen; lasers were used because interferometric phase shift measurements on highly-absorbing films require the use of intense, coherent light sources.

3-2 Preparation of Samples

The samples used in this study were prepared by Dr. A.E. Curzon. Gold films to be used in phase shift measurements were prepared in the following way. A thin film of sodium chloride was evaporated on a microscope slide at room temperature, and a gold film was evaporated on top of the salt layer. The purity of the gold before evaporation was 99.999% or better. The pressure during evaporation was 10^{-5} torr or less. The slide was removed from the evaporator and was immersed in water to dissolve the salt and "float" the gold film, which, supported by surface tension, stayed on the surface of the water. A microscope cover glass with a hole (usually of diameter 1.5 mm to 2 mm) was then brought up from under the film; the film was picked up and the excess water was partly blotted away and the remainder was allowed to evaporate. The result of this procedure was a film suspended over a hole. It was found that a 1000Å-thick film could be suspended over an aperture of diameter up to about 7 mm, but smaller apertures were used for the experiment because films suspended over the larger holes were found to be too fragile to work with conveniently. The reason for making suspended films is that such films permit unambiguous phase shift measurements; a phase shift measurement for a film on a substrate contains an unknown contribution from the substrate unless the thickness of the substrate is precisely known. The

phase shifts could be compared for two films of different thicknesses, mounted on identical substrates, or mounted side by side on the same substrate. Then the thickness of the substrate may remain unknown, but the thickness would have to be very nearly the same under each sample. Rather than attempt to produce uniformly thick substrates, it was decided to use suspended films.

From transmission electron diffraction studies at oblique incidence, performed by Dr. Curzon, it was concluded that the films were highly polycrystalline--no anisotropy was observed in the diffraction pattern. The crystallite size, estimated from electron micrographs, was of the order 100Å to 1000Å. The films were examined visually under a microscope, and those films with obvious defects (wrinkles or pinholes) were rejected.

The suspended films were used for phase shift measurements. The same films could also have been used for transmissivity measurements. It was easier, however, to make the transmissivity measurements on films on substrates, because it was then possible to use larger beam diameters. The effect of the substrate on the measured transmissivity will be discussed later. The films used in transmissivity measurements were evaporated directly on glass microscope cover slips at the same time that the films to be "floated" were evaporated. This ensured that the transmissivity and phase shift measurements were made on films of the same thickness. A small

difference in thickness could arise from the difference in orientation of the slides in the evaporator, but this effect was made negligibly small by placing the slides close to each other and reasonably far away from the source. Small differences in thickness could also arise from the difference in the substrate materials; a gold film vacuum-deposited on glass will not necessarily have the same thickness as a gold film simultaneously deposited on salt, because the sticking coefficients for the two substrate materials could be different. However, this effect is negligible for films thicker than approximately 100Å, because only the initial nucleation rates would be different; as soon as a layer of gold is present on both surfaces, the sticking coefficients become the same.

3-3 Measurement of Film Thicknesses

The gold films used in this study had thicknesses in the range 170Å to 1800Å. The thicknesses of the films were determined using the following three independent methods.

3-3-1 Thickness Measurement by Weighing

Each thickness measurement included placing a pre-weighed piece of mica adjacent to the other two slides in the evaporator and weighing it again after deposition of the gold film. The difference in weights was presumed to be the weight of the film. The area of the film was measured, and the thickness was then calculated according to

$$d = \frac{V}{A} = \frac{M}{DA} \tag{73}$$

where d, V, A, M, and D are, respectively, the thickness, volume, area, mass, and density of the film. The density of the film was assumed to be the same as the bulk density of gold, 19.32 gm/cm^3. Thèye (1970) indicates that this assumption is justified except for very thin films (d < 200Å). The area of each film was approximately 1 cm^2 and the weighing was done using a Cahn Model G2 Electrobalance with a maximum sensitivity of $5 \cdot 10^{-8}$ gm. The uncertainty in thicknesses determined by this technique was approximately ±5%. The weighed film would have a slightly different thickness from the other two films produced in the same evaporation, due to

the difference in orientation of the substrates in the evaporator, but this effect was made negligible as before.

3-3-2 Thickness Measurement Using Frequency Shift of Crystal Oscillator

A Sloan Model DTM-4 Thickness Monitor was also used to determine the thicknesses of the films. The basic component of this device is a quartz crystal resonant at 5 MHz. This crystal was placed in the evaporator, adjacent to the substrates on which the films to be studied were to be deposited. When a film was deposited, the addition of mass to the crystal produced a change in its resonant frequency. This frequency change was measured, and the film thickness was then calculated, using the observation that the change in frequency was proportional to the mass (or thickness) of the film deposited. When the crystal was carefully calibrated, thicknesses determined by this technique were accurate to within ±5%.

3-3-3 Thickness Measurement Using Fizeau Fringes

The previous two methods of thickness measurement were used for all of the films. A third method, using a Sloan Model M-100 Ångstrometer, was also applied for some of the films. This method (Françon, 1966, p. 275; Heavens, 1965, p. 106) consisted of taking a gold film previously vacuum-deposited on a glass slide, and depositing an additional layer, approximately 1000Å thick, of aluminum (or silver, or

any highly-reflecting material) on top of the gold film and the bare substrate beside the gold film. The region of bare substrate was provided by placing a mask over part of the slide during evaporation of the gold film. The resulting glass-gold-aluminum sandwich is illustrated schematically in cross-section in Figure 2. These thickness measurements were of course performed after completion of the transmissivity measurements.

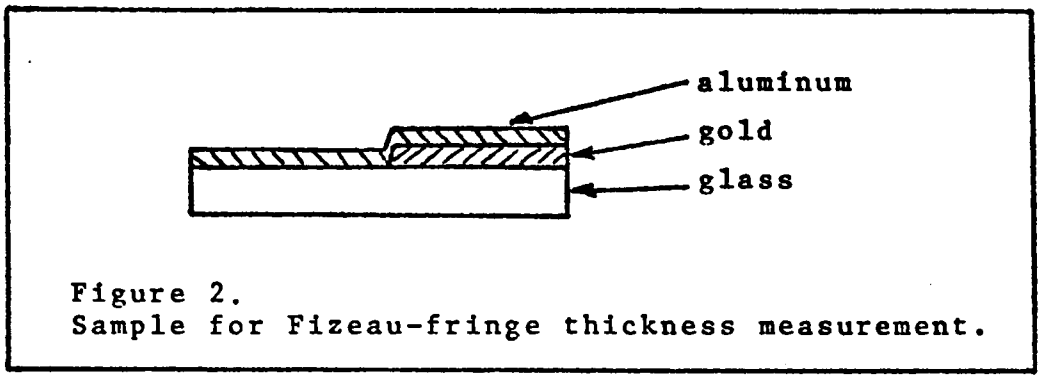

Figure 2.
Sample for Fizeau-fringe thickness measurement.

The specimen thus produced was then used as one of the plates in a wedge arrangement illuminated with sodium light. The plates were adjusted for approximate parallelism, but with a small wedge angle, and the resulting fringe pattern, consisting of narrow dark lines on a bright background (Figure 3) was photographed.

The region of interest was the step at the edge of the gold film; this step appeared as a discontinuity in the fringe pattern, with a jump of one fringe corresponding to a difference in thickness of half a wavelength of sodium light, or 2946Å. In order to be able to see which fringe should be

associated with any particular fringe on the other side of the

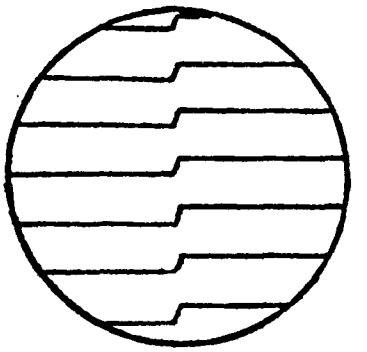

Figure 3.
Measurement of film thickness using Fizeau fringes. This fringe pattern corresponds to a step of approximately 1000Å (λ=5893Å).

discontinuity, the step was not allowed to be too sharp. This was accomplished by keeping the mask approximately 1 mm from the surface of the slide during evaporation of the gold film.

The major limitation on this thickness-measuring technique was the width of the fringes. The reflectivity of the plates should be high, the separation of the plates should be small, and the linewidth of the source should be narrow, to produce narrow fringes and maximum accuracy. The accuracy obtained in our thickness measurements using this technique was approximately ±100Å.

All three methods of thickness measurement yielded, within their respective accuracies, results in agreement with one another. The crystal oscillator method was the most accurate method for films with thicknesses up to approximately 2000Å; for greater thicknesses, the other methods were more accurate.

In addition to the three methods of thickness measurement, the frequency shift of the quartz crystal was plotted against (a) the total mass of gold evaporated, and (b) the mass deposited per unit area, with the same geometry for each evaporation. Both of these studies yielded points along straight lines, indicating that the mass deposited per unit area was proportional to the mass evaporated. This gave an additional check on the relative thicknesses of the films, since the mass evaporated was accurately known in each case.

Another method for measuring the thickness of a thin film involves shining a monochromatic beam of x-rays on the film at various angles of grazing incidence, and studying the resulting interference pattern (Croce, Devant, Sere, and Verhaeghe, 1970; Croce, Gandais, et Murraud, 1964; Mozzi and Guentert, 1964, p. 79; Wainfan, Scott, and Parratt, 1959, p. 1608; Parratt, 1954; Kiessig, 1931). Thèye (1970, p. 3061) has reported that the method can yield thickness measurements accurate to within 1%. This method was not used here; it is time-consuming and cannot be conveniently used on films thicker than a few hundred Ångstroms.

3-4 Principle of the Measurement of Optical Constants Using Transmission Interferometry

In principle, the transmissivity and the phase change on transmission can be ascertained by placing the sample in one arm of a Mach-Zehnder interferometer, as illustrated in Figure 4, and noting the change in the amplitude and phase of the recombined beam as the sample is inserted or withdrawn.

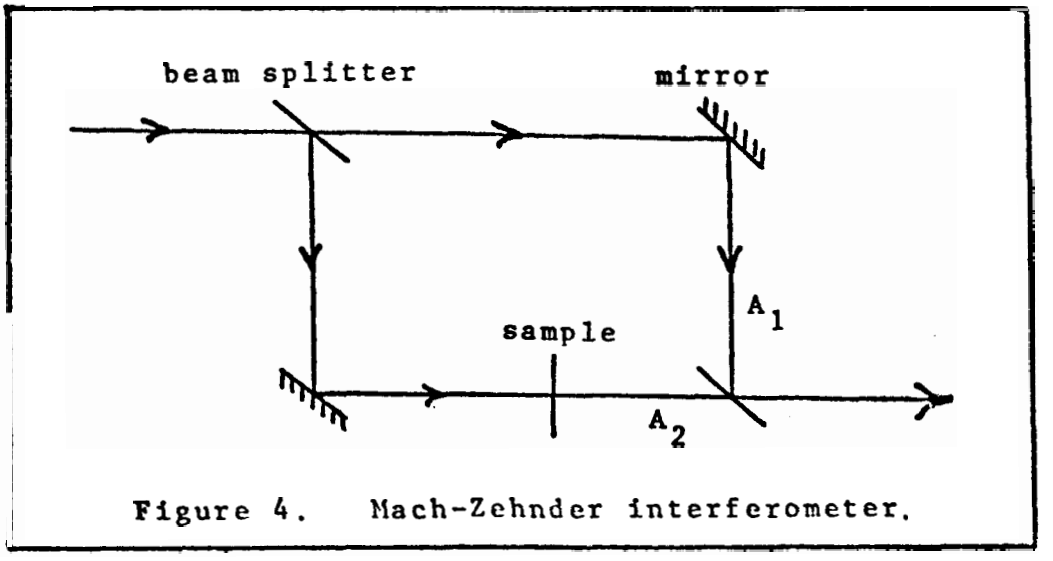

Figure 4. Mach-Zehnder interferometer.

If ψ is the observed phase shift resulting from insertion of the sample, η is the phase change across a thickness of air equal to the thickness d of the sample $\left(\eta = \frac{2\pi d}{\lambda_o}\right)$, and γ is the phase change on transmission through the sample, the following relation holds:

$$\psi = \eta - \gamma \quad , \tag{74}$$

since the measured phase shift is the phase difference produced by displacing air with the sample.

If the amplitudes of the two beams in the interferometer are A_1 and A_2, the intensity of the recombined beam is given by (Klein, 1970, p. 184):

$$I \alpha A_1^2 + A_2^2 + 2A_1A_2 \cos\theta, \qquad (75)$$

where θ is the phase difference between the beams. Thus it is possible to determine both the transmissivity and the phase change on transmission simultaneously, by studying the change in intensity and phase of the recombined beam when a sample is replaced by another sample of different thickness. We have chosen, however, to separate the transmissivity and phase shift measurements into two independent experiments, because, although we can, in principle, determine the transmissivity from the same data that determine the phase shift, the transmissivity is more easily and more accurately determined by a separate measurement when the transmissivity is very small. This will be discussed in detail at the end of section 3-5-4.

3-5 Phase Shift Measurement

3-5-1 Description of the Interferometer

In performing the phase shift measurements, it was found desirable to have some means for taking into account the slowly-varying drifts in the phase of the recombined beam when the interferometer was used in air. Accordingly, the arrangement of optical components for the phase shift measurements was as illustrated in Figure 5. For vibration isolation, the apparatus was positioned on a heavy granite slab resting upon polyurethane foam. The interferometer was also enclosed in a box to reduce the effects of air currents. An air system was used because the added experimental complexity of enclosing the interferometer in an evacuated chamber was not deemed justifiable at this early stage of development of the technique.

The incident laser beam was split into two reflected beams and one transmitted beam by means of a glass plate (beam splitter #1) approximately 6 mm thick. Beams from additional reflections were present, but were not used. The intensity of the transmitted beam was approximately 90% of the intensity of the incident beam. The transmitted beam passed through a chopper (described in greater detail in section 3-5-2), was reflected by a right-angle prism, and was split again by another glass plate (beam splitter #3) which had a transmissivity of approximately 90%. The transmitted beam was then

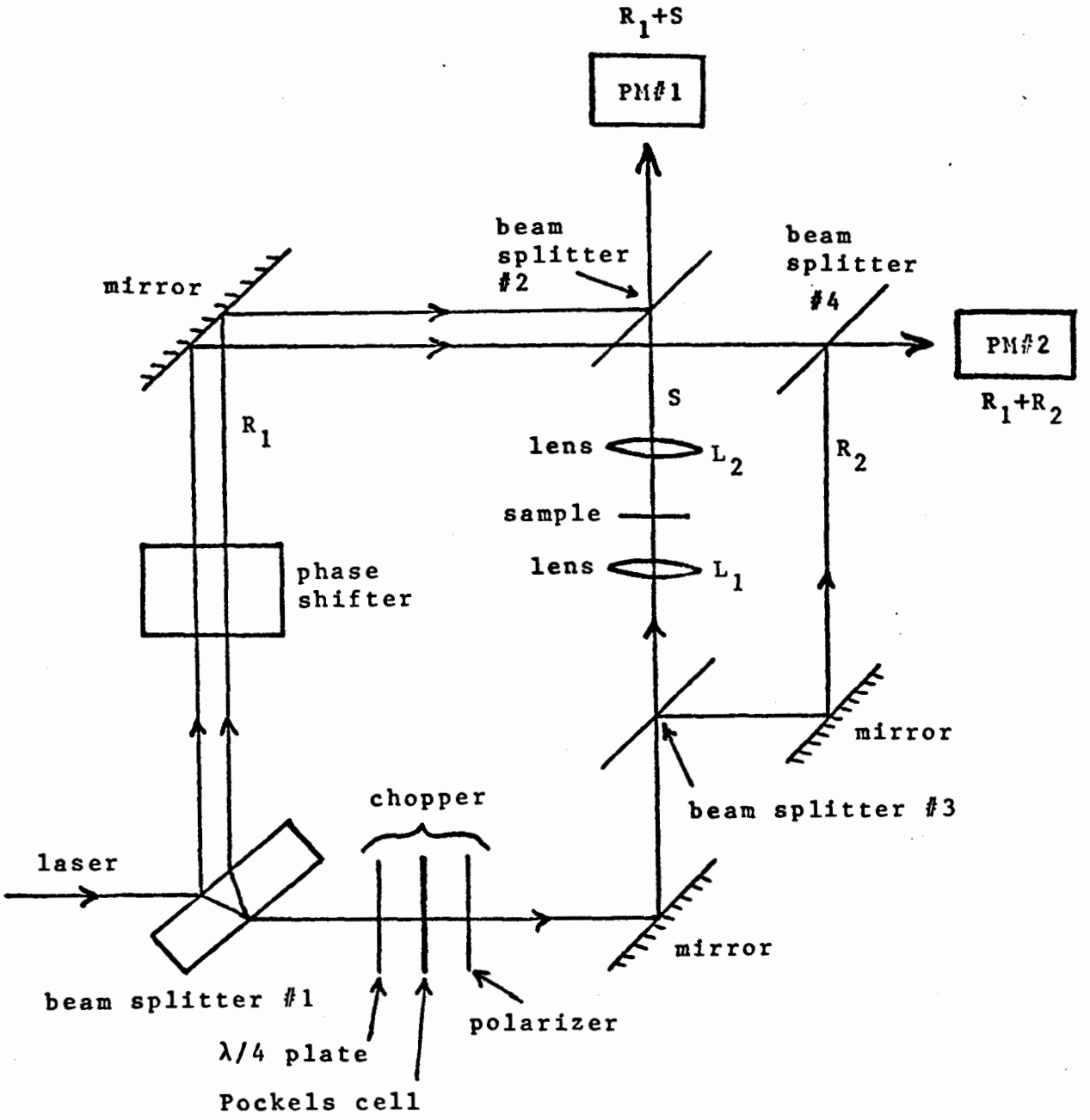

Figure 5. Apparatus for phase shift measurement.

focussed on the sample by lens L_1 and re-collimated by lens L_2. The sample was not placed precisely at the focus but at a position such that the beam diameter at the sample was approximately 1 mm. The beam incident on the sample was not exactly a plane wave, but was near enough plane to preserve with reasonable accuracy the validity of the equations applicable to plane waves. Only a small part of the center of the re-collimated (and expanded) beam was used--the divergence of the corresponding part of the beam at the sample was of the order of one milliradian. The beam from the sample was recombined at beam splitter #2 with one of the two beams reflected from beam splitter #1. It was convenient to adjust the position of the collimating lens L_2 so that the beam emerging from lens L_2 was slightly divergent; when the recombined beam (the "sample beam") was displayed on a screen, a pattern of concentric fringes was then observed. These fringes could be tuned for any convenient spacing by appropriate adjustments of the optical alignment. The center of the fringe pattern was directed onto a small aperture behind which was located a photomultiplier (denoted PM#1 on Figure 5). The ratio of the diameter of the aperture to the spacing of the fringes was small, for high phase resolution, but not so small that intensity was lost unnecessarily.

A phase reference was provided by an optical shunt around the sample; this beam was recombined with the other of the two beams reflected from beam splitter #1. The reason

for having two beams reflected from beam splitter #1 was that this configuration avoided the possibility of "mixing" beams S and R_2; such mixing could have occurred if the same beam were recombined with both S and R_2. The resulting fringe pattern for this "reference beam" was a series of straight, parallel fringes which could be adjusted for large separation. This pattern was directed onto a small aperture situated directly in front of a photomultiplier (denoted PM#2 on Figure 5).

3-5-2 Chopper

The chopper consisted of three components: a quarter-wave plate, a Baird-Atomic Model JT-3 Pockels cell, and a polarizer. The quarter-wave plate was oriented with its axis at 45° to the plane of polarization of the laser beam, producing circularly polarized light. This beam then passed through the electro-optic modulator or Pockels cell, which, when driven by a voltage varying periodically in time, produced elliptically polarized light with the amplitude of the vertical component of the electric field also varying periodically in time. This component was transmitted by the polarizer. The result was that the emergent light was plane-polarized and was amplitude-modulated (or intensity-modulated). The chopping frequency used was approximately 1500 Hz, because this happened to be the resonant frequency of an ignition coil used as a step-up voltage transformer. A mechanical chopper, such

as a rotating wheel containing slots, could achieve essentially the same result as the electro-optic modulator, but produced undesirable vibration and air currents, to which the interferometer proved to be very sensitive.

3-5-3 Phase Shifter

The interferometer was scanned in phase by means of a phase shifter consisting of an evacuable cell having a path length of approximately 1 cm. To operate the phase shifter, the cell was evacuated and nitrogen gas was then allowed to leak slowly through a flow regulator into the cell, which was connected to a large-volume reservoir. The increase in pressure caused an increase in the optical path length in the cell. The result was that the phases of the beams at both photomultipliers were slowly changed. The pressure-scanning cell had the desirable property that it changed the phase of the transmitted beam without significantly altering the intensity or the state of polarization of the beam. Furthermore, the range of phase over which the device could scan was easily controlled by choosing the appropriate combination of gas and path length. If, for example, it had been desired to scan accurately in phase over a small range, helium gas in a shorter path length could have been used. In our case, the range was about 4 wavelengths in optical path difference, or 8π radians in phase.

3-5-4 Electronics

The arrangement of electronic apparatus was as illustrated in Figure 6. The signals from the two photomultipliers were detected by two Princeton Applied Research Model HR-8 lock-in amplifiers and were displayed on a 2-pen chart recorder. When the phase shifter was operated, the recorder output was of the form illustrated in Figure 7. The chart displayed two traces, one corresponding to the beam transmitted through the sample and the other corresponding to the reference beam which bypassed the sample. Since the chopper was in the "sample arm" of the interferometer, and electronic phase-sensitive detection was used, the large d.c. component arising from the reference beam denoted by R_1 in Figure 5 was rejected. This facilitated amplification of the desired a.c. signal component.

From equation (75), the intensities at photomultipliers #1 and #2 were given by

$$I_1 \propto R_1^2 + S^2 + 2R_1 S\cos\theta_1 \qquad (76)$$

and

$$I_2 \propto R_1^2 + R_2^2 + 2R_1 R_2\cos\theta_2 \quad , \qquad (77)$$

where R_1, R_2, and S were the amplitudes of the beams as indicated in Figure 5, θ_1 was the phase difference between beams R_1 and S, and θ_2 was the phase difference between beams R_1 and R_2.

Beams S and R_2 were chopped at an angular frequency f.

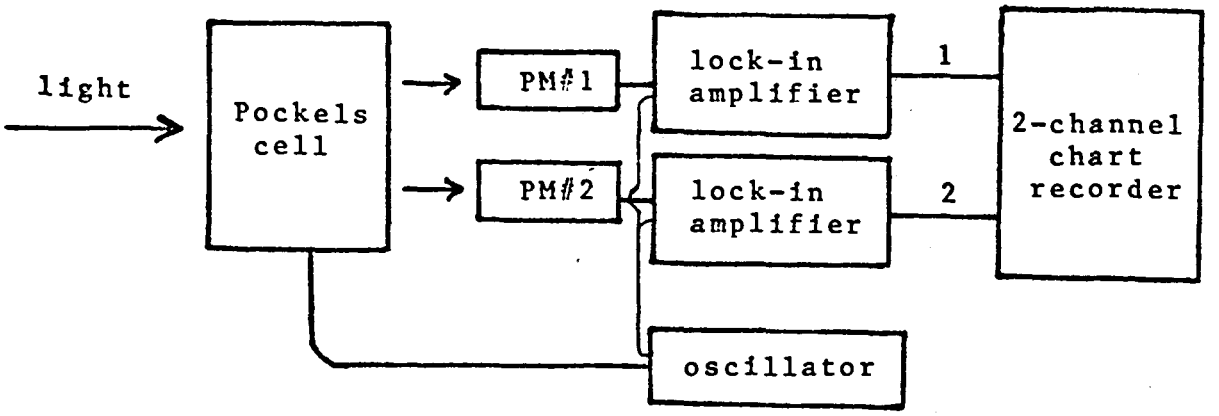

Figure 6.
Block diagram of arrangement of electronic apparatus.

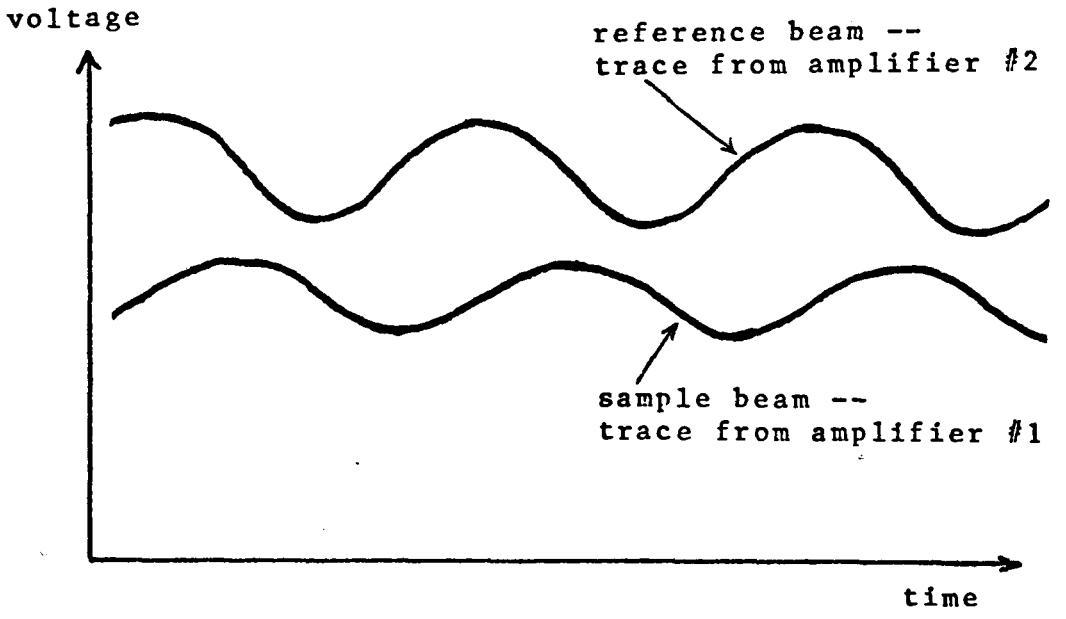

Figure 7. Chart recorder output.

Let

$$S = S^1 + s \cos ft \quad (\text{where } S^1 \geq s) \tag{78}$$

and

$$R_2 = R_2^1 + r_2 \cos ft \quad (\text{where } R_2^1 \geq r_2). \tag{79}$$

Then

$$I_1 \propto R_1^2 + (S^1)^2 + s^2\cos^2 ft + 2S^1 s \cos ft + 2R_1 S^1 \cos\theta_1 + 2R_1 s \cos ft \cos\theta_1 \tag{80}$$

and

$$I_2 \propto R_1^2 + (R_2^1)^2 + r_2^2\cos^2 ft + 2R_2^1 r_2 \cos ft + 2R_1 R_2^1 \cos\theta_2 + 2R_1 r_2 \cos ft \cos\theta_2. \tag{81}$$

Only the signal components at the chopping frequency were measured. The output voltages of the lock-in amplifiers were thus

$$V_1 \propto s(S^1 + R_1\cos\theta_1) \tag{82}$$

and

$$V_2 \propto r_2(R_2^1 + R_1\cos\theta_2). \tag{83}$$

When a highly-absorbing sample was in the beam, S^1 in equation (82) was small compared to R_1, so the amplitude of the ripple on trace #1 in Figure 7 was large compared to the d.c. level. If no sample was in the beam, the amplitude of the ripple on trace #1 was smaller than the d.c. level.

In any case, the amplitude of the ripple on trace #1 was proportional to the amplitude of the beam transmitted through the sample. This made it possible, in principle, to measure

both the change in amplitude and phase simultaneously, as mentioned in section 3-4. The reason for not doing this was that very slight beam displacements produced large changes in intensity at the photomultiplier (PM#1 in Figure 5); such beam displacements unavoidably occurred when attempts were made to calibrate the change in amplitude using thick neutral density filters. If calibrated attenuators with thicknesses comparable to those of the films being measured had been available, the experiment could have been conducted by measuring both the change in amplitude and phase simultaneously, because the thin films did not produce noticeable beam displacements. The calibration could have been omitted if films had been compared only in a small thickness range, but this would have required greater accuracy in thickness measurements. For the phase shift measurements, it was desirable to compare films of greatly different thickness, to maximize the measured effect, but intensity or amplitude measurements on films of considerably different thickness require calibration of the photomultiplier response. Because of these difficulties, it was decided to measure the phase shift and the transmissivity in two independent experiments.

Having decided to make the transmissivity measurements independently, we decided also to make these measurements using films on substrates. The suspended films used for phase shift measurements could also have been used for the transmissivity measurements, but it was found that transmis-

sivity measurements on such small samples were difficult to perform. For example, diffraction at the edges of the apertures over which the samples were suspended could lead to serious photometric errors. Furthermore, the presence of a glass substrate has a negligible effect on the transmissivity if a sample of large area is used (see section 3-6).

3-5-5 Details of the Phase Shift Measurement

A phase shift measurement was made in the following way. With no sample in the beam, gas was admitted to the phase shifter, producing on the chart two traces with some arbitrary phase difference between them. The sample was then inserted in the beam as in Figure 5, and the supply voltage on photomultiplier #1 was increased as necessary and/or the sensitivity of the lock-in amplifier was increased to bring the signal to a measurable level. No adjustment was made to the reference signal from photomultiplier #2, since that signal was completely unchanged by the insertion of the sample. The presence of the sample was the only change in the optical train. The phase shifter was then scanned again, and the change in the phase difference between the traces on the chart was measured. This would be the phase shift due to the sample, if the phase difference between the sample beam and the reference beam had not drifted. In general, the phase shift was only known modulo 2π, of course, but our films were all sufficiently thin that the measured phase shifts were

known to be between zero and 2π.

3-5-6 Compensation for Drifts in Phase

Note that the optical arrangement of Figure 5 automatically compensated for phase drifts arising in the optical components common to both the sample beam and the reference beam. When the apparatus was allowed to monitor the drift, with the phase shifter inoperative or withdrawn from the beam, it was observed that large drifts (several fringes) sometimes occurred over a time interval of approximately one hour. However, these drifts were present in both traces on the chart; the phase difference between the two traces remained unchanged. When the phase shifter was operated, the drift became manifest as variations in the period of the two traces as illustrated in Figure 8.

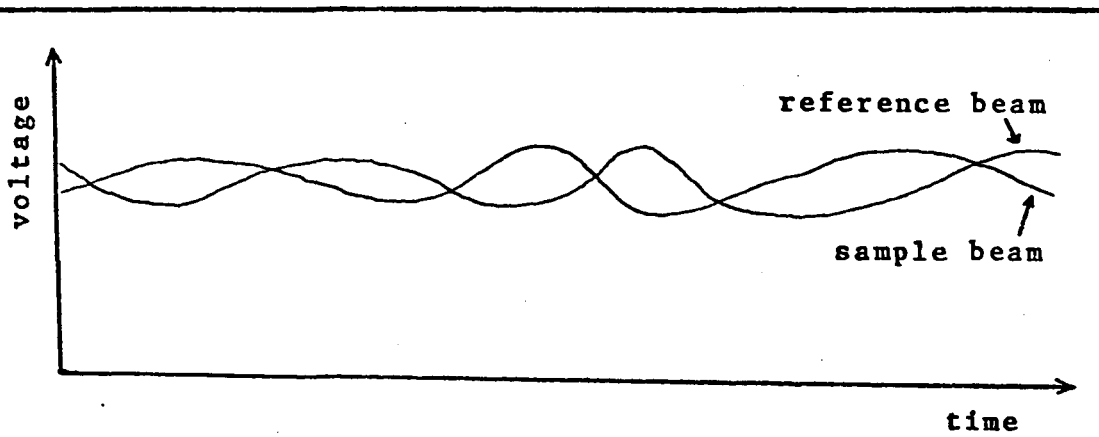

Figure 8.
Effect of phase drift (exaggerated) on chart recorder output. The time scale is such that one cycle corresponds to a few minutes.

Even though the traces were of variable period, the phase difference between them was well defined over each cycle, so that an accurate measurement of this phase difference was possible.

The exact origin of the observed drifts is unknown, but one possibility, for example, could have been that the optical path length in the Pockels cell changed as the cell warmed up or cooled down, depending on its heat-loss rate, which, because of air currents, was probably not constant in time.

A small residual drift of the phase of the sample beam relative to the phase of the reference beam was also observed. This drift could, perhaps, have been due to changes in air temperature, resulting in changes in optical path difference between beams R_1 and S, and between R_1 and R_2. This effect could be minimized by making the geometrical path difference in air nearly the same (with the same sign) in both cases, or, more simply, nearly zero for both. To take this drift into account, the phase shift measurements were repeated several times with the sample alternately in and out of the beam. The resulting measurements were than plotted as illustrated in Figure 9. The difference in phase between the two resulting curves was the phase shift due to the sample.

One could, of course, have made a direct measurement of the phase difference between two samples of different thickness, but it was convenient to use a sample of zero thickness (i.e. no sample) as a reference.

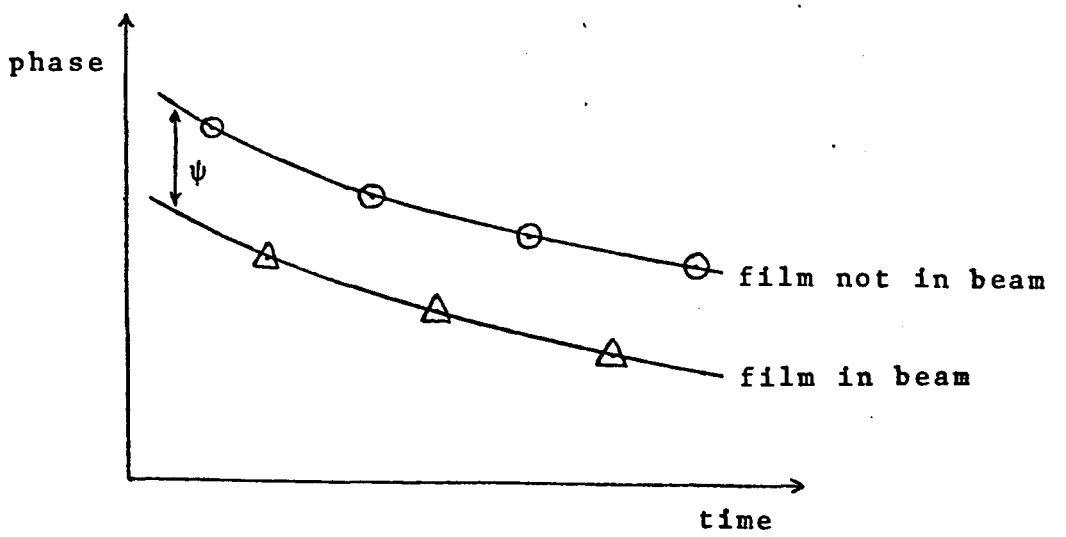

Figure 9.
Phase difference between sample beam and reference beam versus time. ψ is the phase shift due to the film. The time scale spans approximately 70 minutes (10 minutes per point). The ratio of the measured phase shift to the drift in phase was typically of the order illustrated here.

One might attempt to make the phase shift measurements more quickly, to minimize the effects of slowly-varying drifts. This did not seem feasible, however, since rapidly-varying drifts from air currents and signal fluctuations from electronic noise were also present, especially when looking at a weak signal from light transmitted through a thick film. These fluctuations were averaged using integrating time constants of the order of 1 second in the output circuits of the HR-8 amplifiers. For a measurement of phase difference versus time, approximately 10 minutes per experimental point represented the optimum.

3-6 Measurement of Transmissivity

The optical density, defined by

$$O.D. = \log_{10} \frac{1}{T} , \tag{84}$$

where T is the transmissivity, was measured at various wavelengths for each film by comparing the intensity of a laser beam transmitted through the film with the transmitted intensity when the film was replaced by various filters of known optical density. The arrangement of apparatus was as illustrated in Figure 10.

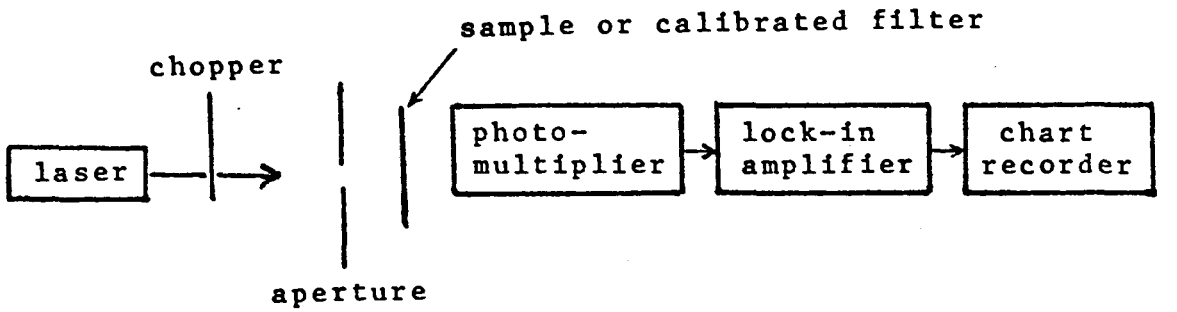

Figure 10.
Apparatus for transmissivity measurement.

The samples for these measurements were gold films of various thicknesses deposited on glass microscope cover slides. These slides were, fortuitously, sufficiently wedge-shaped in cross-section that it was possible to use a large enough beam diameter (up to 1 cm) to permit averaging over several fringes arising from interference within the substrate, thereby reducing the change in transmissivity introduced by the sub-

strate-air interface to a small contribution (approximately 4%). Variations in transmissivity among cover glasses were found to be negligible. Since k was determined (as will be described in Section 4-2-2) using only the thickness dependence of the transmissivity, the effect of the substrate was inconsequential.

CHAPTER 4

EXPERIMENTAL RESULTS

4-1 Data

The measured optical densities and phase shifts at various wavelengths for gold films of various thicknesses are listed in Table I. Films on glass substrates were used for optical density measurements, and suspended films were used for phase shift measurements. A measured phase shift was the phase shift [ψ in Figure 9 and in equation (74)] introduced by inserting a sample into the beam.

Some of the measurements were repeated after storing the samples in a dessicator for two months; no aging effect was observed.

The stated optical density and phase shift values are averages of measurements repeated on several different samples of the same thickness (from the same evaporation). The error estimates on these values generally correspond to approximately one standard deviation on each side of the mean. In some cases, the number of measurements was too small (3 or 4, for example) for the standard deviation to be of statistical significance, and in these cases the error estimates simply indicate the entire range of measured values. The error estimates on the optical density measurements indicate the extent of reproducibility in calibration, rather than

Table I. Measured Optical Densities (O.D.) and Phase Shifts (ψ) versus Thickness for Gold Films

Film thickness (Å) ±5%	λ_o = 6328Å O.D. ±0.1	λ_o = 6328Å ψ (degrees) ±5°	λ_o = 5145Å O.D. ±0.2	λ_o = 5145Å ψ (degrees) ±10°	λ_o = 4880Å O.D. ±0.2	λ_o = 4880Å ψ (degrees) ±10°
168	0.40	40	---	---	---	---
252	0.70	55	---	---	---	---
412	1.15	70	0.90	29	0.90	10
644	1.80	79	---	---	---	---
764	2.15	86	1.45	41	1.50	---
870	2.55	92	---	---	---	---
1076	3.15	99	2.05	50	2.00	5
1300	3.90	110	2.45	46	2.40	---
1800	---	---	3.70	66	3.45	12

necessarily indicating deviations in optical density among different samples. Similarly, the error estimates on the phase shift measurements are largely due to the finite phase resolution of the interferometer, and do not necessarily indicate deviations among different samples. The interferometer had poorer phase resolution at 4880Å and 5145Å than at 6328Å, because the fringe contrast was better with the helium-neon laser than with the argon laser. This effect was presumably due to the fact that the linewidth of the helium-neon laser was less than that of the argon laser.

4-2 Determination of Optical Constants in the Thick-film Limit

The optical constants n and k were determined independently, using only the slopes of the "best" straight lines drawn through the experimental points in the range of thicknesses where multiple reflections could be ignored. This range of thicknesses can be found experimentally by noting the thickness above which the optical density or phase shift appears to change linearly with thickness. This range can also be calculated, if k is approximately known in advance, by using the criterion that multiple reflections can be ignored if

$$e^{-\frac{4\pi k d}{\lambda_o}} \ll 1 \quad .$$

We chose the criterion that a film was considered thick enough if

$$e^{-\frac{4\pi k d}{\lambda_o}} < 3\%. \qquad (85)$$

The errors resulting from this approximation were smaller than the error estimates on the measurements. A more stringent criterion would result in data being unnecessarily discarded. From (85) it follows that

$$\frac{d}{\lambda_o} > \frac{\ln\left(\frac{100}{3}\right)}{4\pi k} \qquad (86)$$

is an equivalent criterion defining the thick-film limit. Using Johnson and Christy's (1972) values of k for gold, we obtain:

$$\left.\begin{array}{l} \lambda_o = 4880\text{Å} \\ \lambda_o = 5145\text{Å} \end{array}\right\} \Rightarrow d \gtrsim 760\text{Å}$$
$$\lambda_o = 6328\text{Å} \quad \Rightarrow d \gtrsim 500\text{Å} . \qquad (87)$$

Only measurements on films satisfying this thick-film criterion were used in determining the optical constants. The reason for doing this is that this technique eliminates surface effects (see below). Since 644Å was the thickness of the thinnest film satisfying (87) for $\lambda_o = 6328\text{Å}$, the films used at this wavelength satisfied the criterion $e^{-\frac{4\pi kd}{\lambda_o}} \leq 1\%$.

4-2-1 Determination of n

In the thick-film limit, the phase changes ϕ_1 and ϕ_2 at the surfaces become constant (independent of thickness), and the phase change on transmission can be written

$$\gamma = \phi_1 + \phi_2 + \frac{2\pi nd}{\lambda_o} . \qquad (88)$$

In this limit, the phase shift ψ is, from equation (74), of the form

$$\psi = \frac{2\pi d}{\lambda_o} - \gamma$$

$$= (1-n)\frac{2\pi d}{\lambda_o} - \phi_1 - \phi_2 . \qquad (89)$$

The rate of change of phase shift with thickness is

$$\frac{d\psi}{d(d)} = \frac{2\pi}{\lambda_o}(1-n) . \qquad (90)$$

n was determined at each wavelength from the slope $\frac{d\psi}{d(d)}$ of the experimental plot of phase shift versus thickness according to

$$n = 1 - \frac{\lambda_o}{2\pi} \cdot \frac{d\psi}{d(d)} \quad , \tag{91}$$

which is equivalent to (90). The slopes were determined using the method of least squares, utilizing only data from films satisfying the thick-film criterion (87). A representative plot is shown in Figure 11.

Figure 11.
Determination of n from the slope of the experimental plot of phase shift vs. thickness. (λ_o=6328Å)

Experimental points are for gold films.

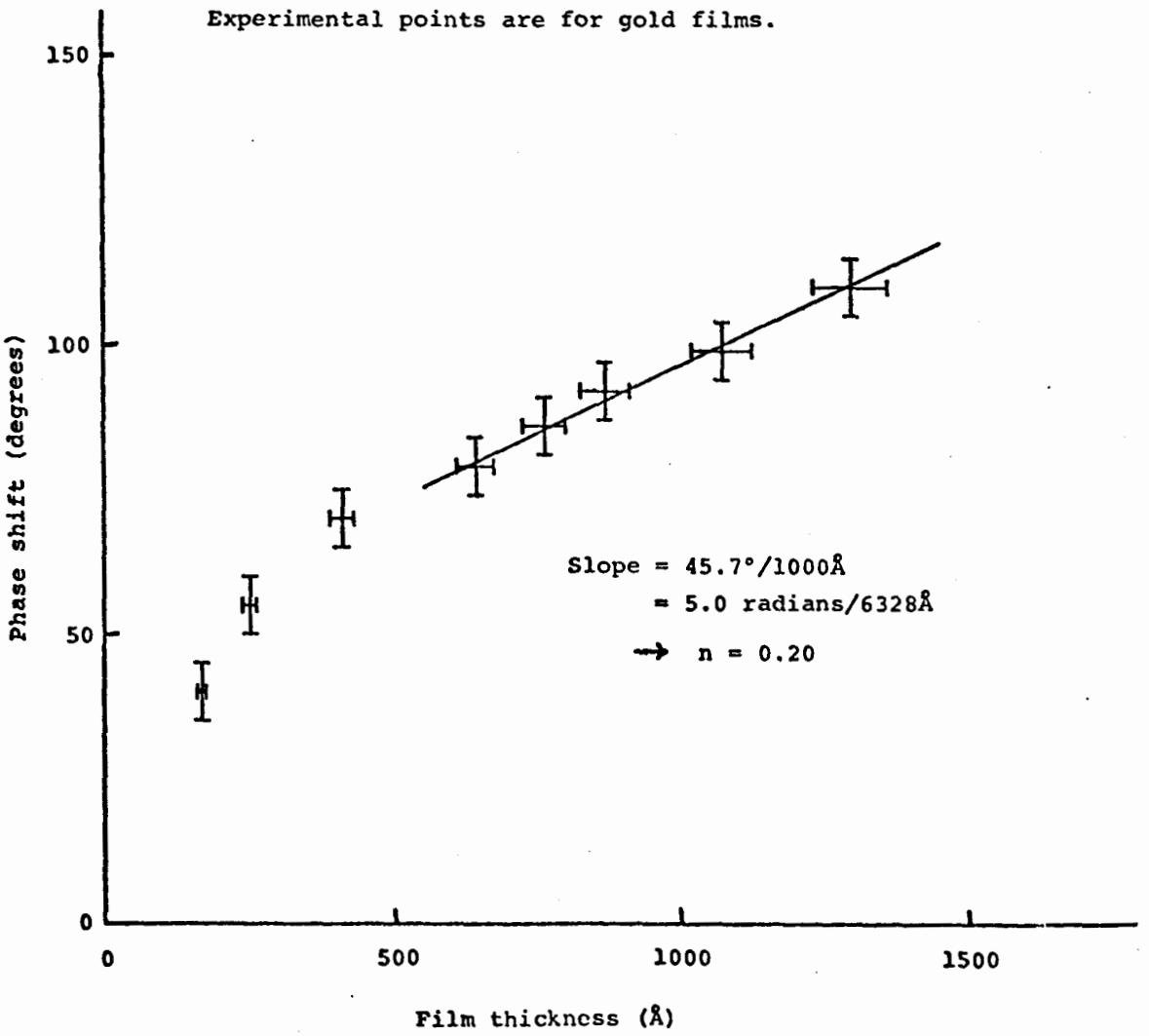

4-2-2 Determination of k

In the thick-film limit, the transmissitivity is approximately

$$T = C\, \bar{e}^{\frac{4\pi kd}{\lambda_o}} , \tag{92}$$

where C is independent of d; thus

$$\log_{10} T = \log_{10} C - \left(\frac{4\pi kd}{\lambda_o}\right)\log_{10} e. \tag{93}$$

Since O.D. = $-\log_{10} T$ from (84), the rate of change of optical density with thickness is, in the thick-film limit,

$$\frac{d(O.D.)}{d(d)} = 0.434 \left(\frac{4\pi k}{\lambda_o}\right) . \tag{94}$$

k was determined at each wavelength from the slope $\frac{d(O.D.)}{d(d)}$ of the experimental plot of optical density versus thickness, using equation (94) in the form

$$k = 2.30 \frac{\lambda_o}{4\pi} \frac{d(O.D.)}{d(d)} , \tag{95}$$

where we have put $\frac{1}{\log_{10} e} \approx 2.30$. The slopes were determined by means of least squares fits to the data from films with thicknesses satisfying the thick-film criterion (87). A representative plot is shown in Figure 12. This method of determining k has been outlined by Heavens (1970, p. 71).

Figure 12.
Determination of k from the slope of the experimental plot of optical density vs. thickness. (λ_o=6328Å)

Experimental points are for gold films.

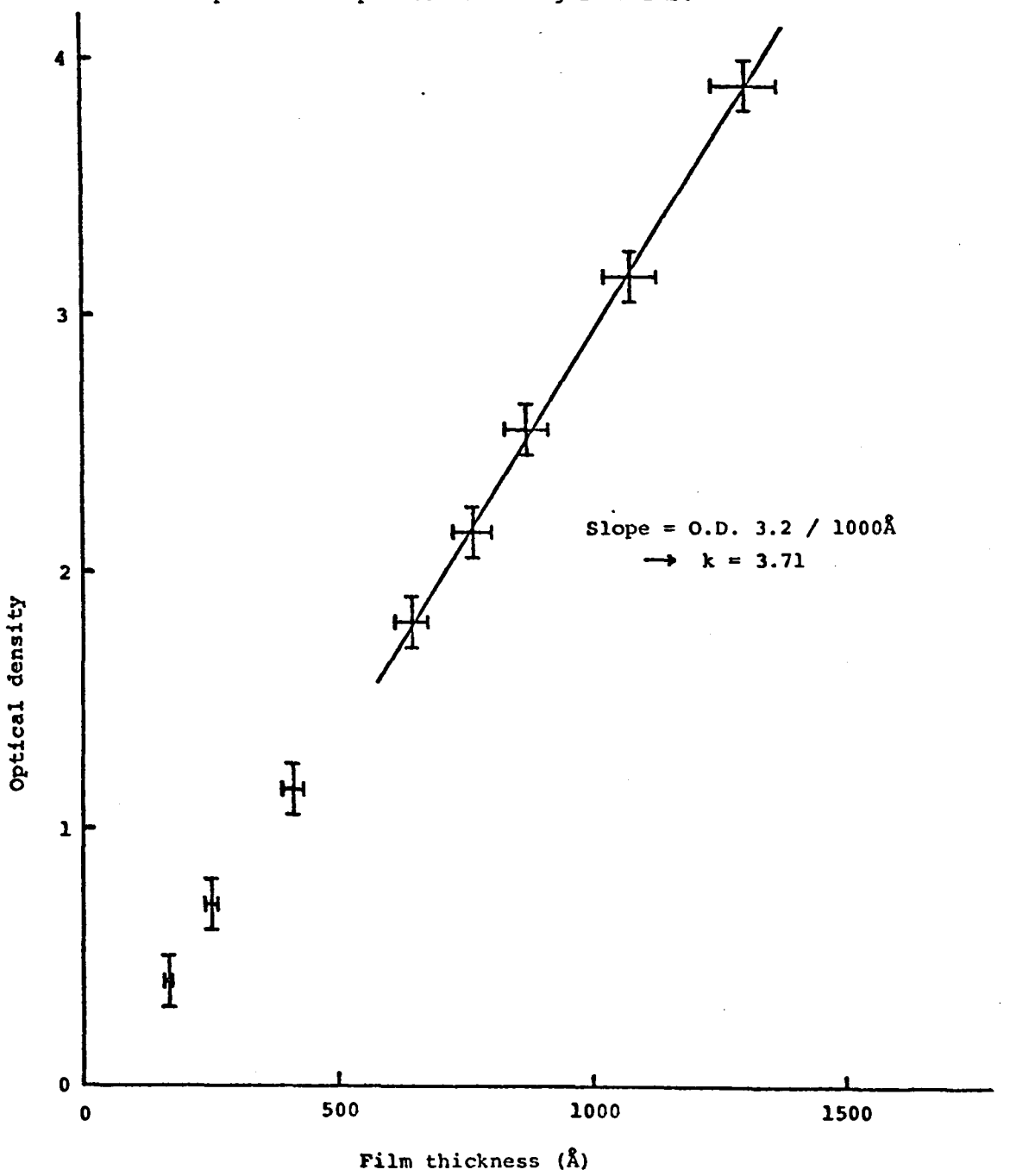

4-2-3 Table of Values of n and k for Gold

Our values of n and k, determined in the thick-film limit in the manner described in sections 4-2-1 and 4-2-2, are listed in Table II. These results represent the "correct" values for n and k in that they are independent of surface conditions.

Table II. Experimental Results for the Optical Constants of Gold, Determined in the Thick-film Limit

λ_o (Å)	n	k
6328	0.20 ± 0.10	3.71 ± 0.25
5145	0.67 ± 0.15	2.05 ± 0.25
4880	0.9 ± 0.3	1.70 ± 0.25

4-3 Comparison of Measurements with the General Theory Incorporating the Effects of Multiple Reflections

The values of n and k determined in the thick-film limit (section 4-2) are the "correct" values because they are determined using only the thickness dependences of the measured optical densities and phase shifts, and surface effects are thus eliminated. (The procedure does require that the surface effects be the same for different samples, and this implies that the samples should have a similar history of preparation.)

The individual measurements of optical density or phase shift must include surface effects. We now wish to compare our measurements with the theory outlined in section 2-2; this theory assumes that the optical constants are the same at the surfaces of the film as in the bulk material. Temporarily making this assumption, we re-determined the optical constants by fitting to the data values of n and k given by the theory in section 2-2. The theory includes the effects of multiple reflections; it is valid for all thicknesses, so measurements on thin films were included in the comparison with the theory. The values of the optical constants determined in this manner deviated from the values determined in the thick-film limit (section 4-2). The extent of the deviations provided an estimate of the surface contributions to the measurements.

We employed equations (64) and (84) to plot theoretical curves of optical density versus thickness (O.D. vs d), and

equations (66) and (74) to plot theoretical curves of phase shift versus thickness (ψ vs d), using a Hewlett-Packard Model 9100 B Calculator, Model 9101A Extended Memory, and Model 9125A Plotter. Since the optical density measurements were performed using films on glass substrates, n_s was put equal to 1.5 in equation (64). The small change in transmissivity introduced by the back surface of the substrate was neglected; the error thus introduced was smaller than the error in the measurements. n_s was put equal to 1 in equation (66) because the phase shift measurements were performed using suspended films.

At a film thickness of zero, the calculated phase shift is zero, of course, and the calculated optical density has a small finite value due to the reflection loss at the boundary of the substrate. In the thick-film limit, the slopes of the theoretical curves approach the values given by equations (90) and (94).

Note that the calculation of each theoretical curve requires the specification of the values of both n and k. To determine n and k at a particular wavelength, the following iterative procedure was employed.

(a) Theoretical curves of O.D. vs d were plotted for various values of k, using the value of n determined in the manner described in section 4-2-1. A representative plot is shown in Figure 13. A new value for k was found by choosing the theoretical curve that provided the best

fit to the experimental points.

(b) Theoretical curves of ψ vs d were plotted for various values of n, using the newly-determined value of k. A representative plot is shown in Figure 14. A new value for n was found by choosing the theoretical curve best fitting the experimental points.

(c) Using the new value of n, O.D. vs d was plotted and k was re-determined. A representative plot is shown in Figure 15.

(d) Using the new value of k, ψ vs d was plotted and n was re-determined. A representative plot is shown in Figure 16.

Steps (c) and (d) were repeated until the values of n and k remained unchanged.

Figure 13.

OPTICAL DENSITY VS. THICKNESS
for n = 0.20 and λ_o = 6328Å.

Experimental points
are for gold films.

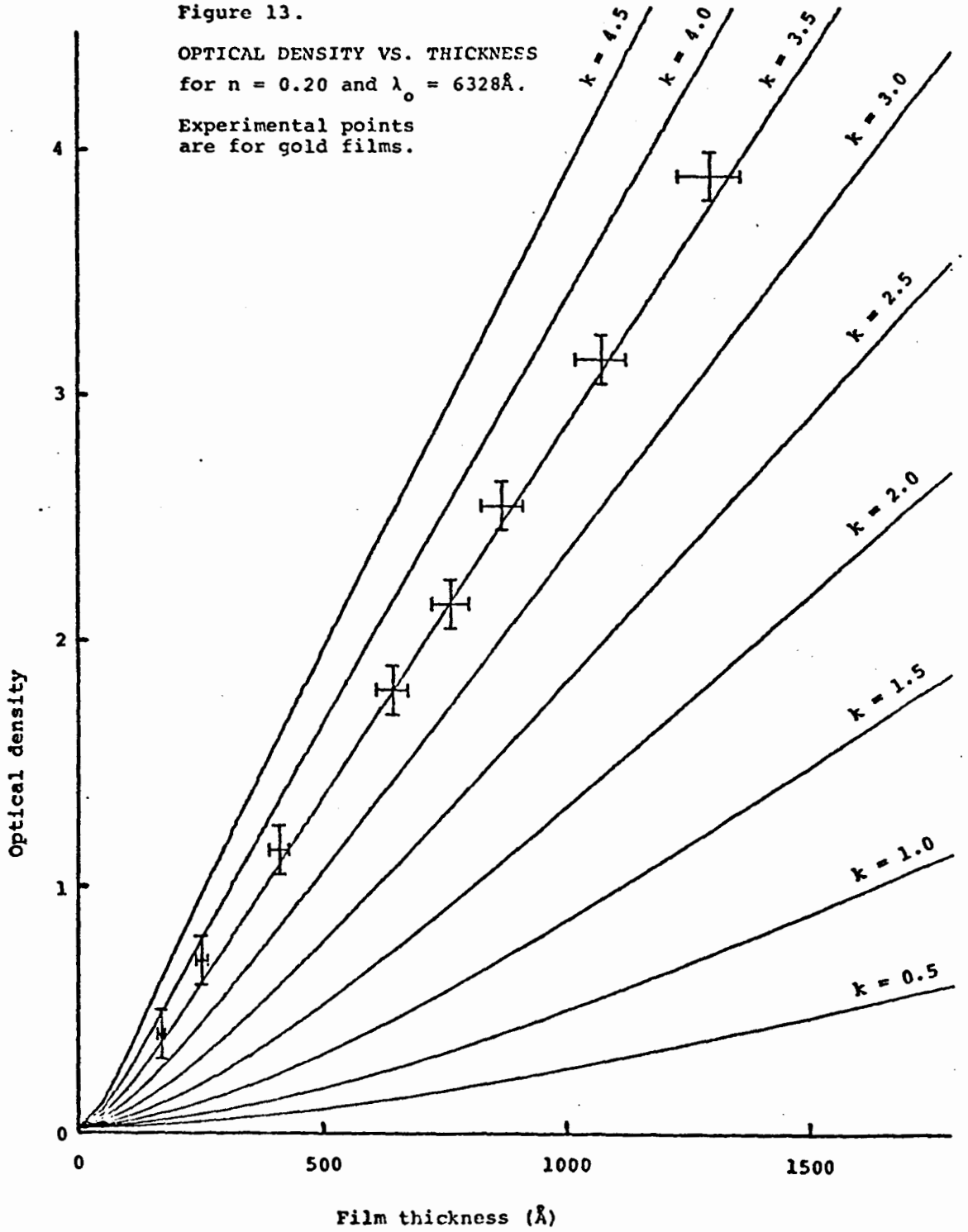

Figure 14.

PHASE SHIFT VS. THICKNESS
for k = 3.7 and λ_o = 6328Å.

Experimental points are for gold films.

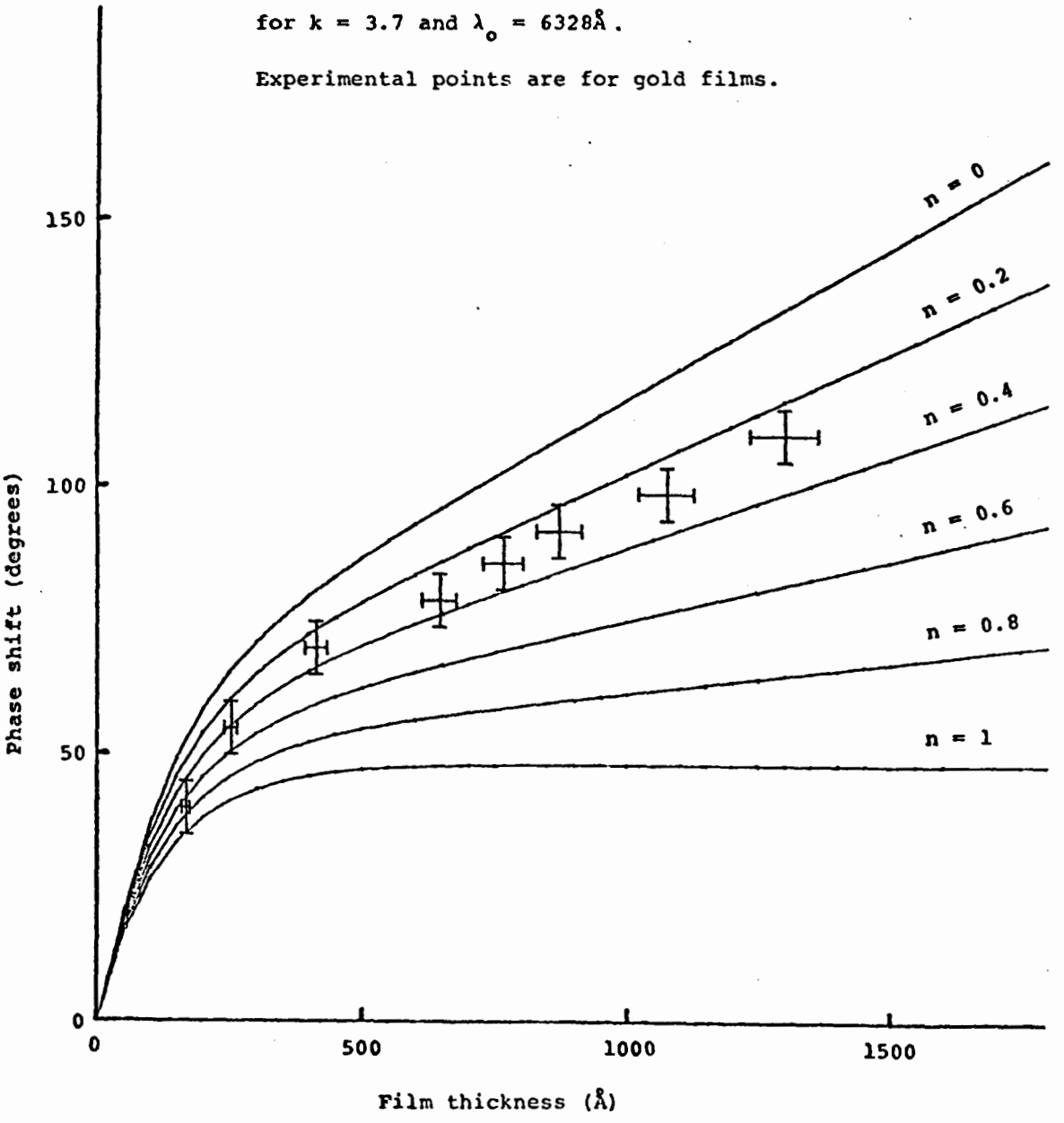

Figure 15

OPTICAL DENSITY VS. THICKNESS
for n = 0.27 and λ_o = 6328Å

Experimental points
are for gold films.

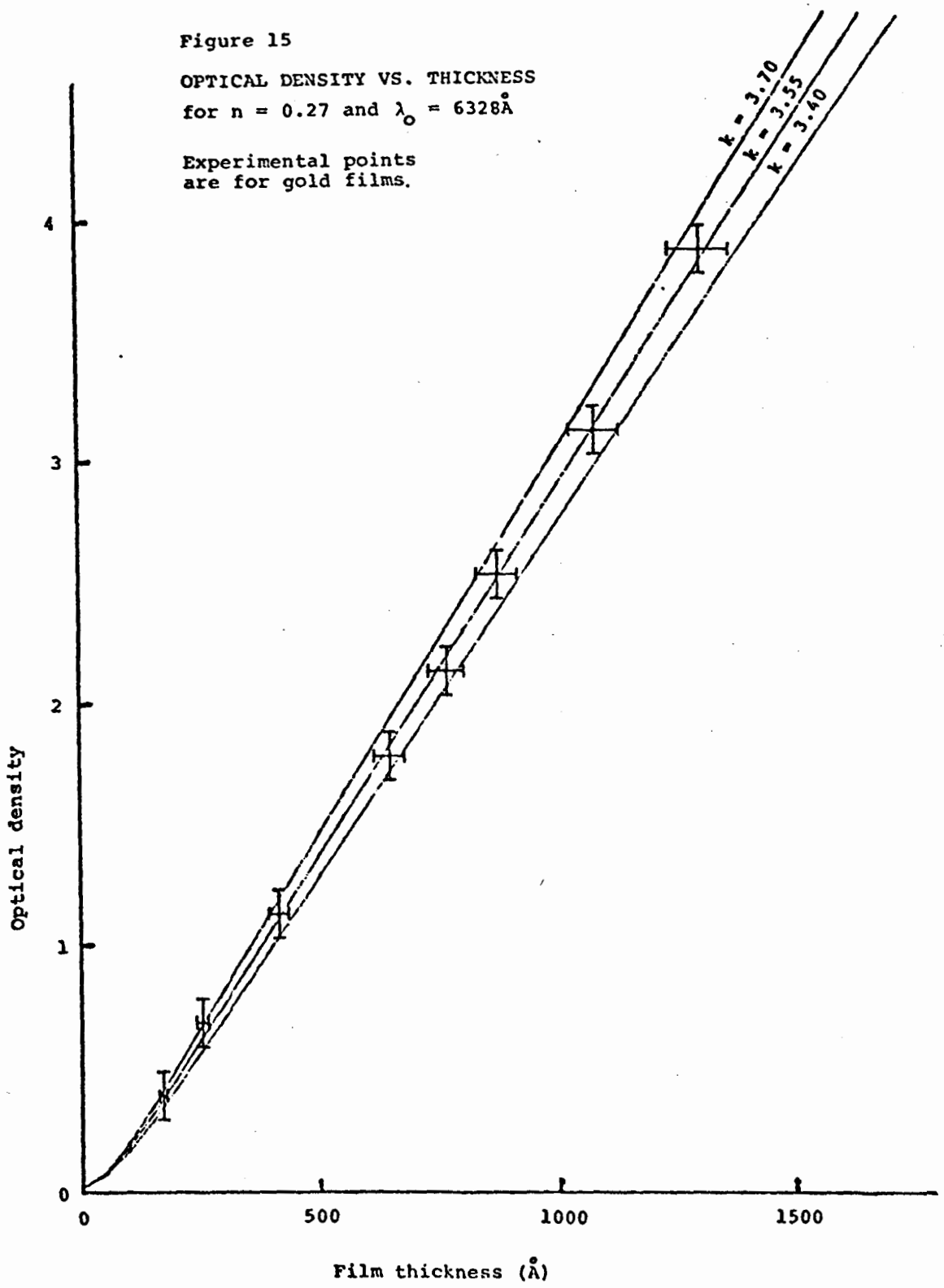

Figure 16

PHASE SHIFT VS. THICKNESS
for k = 3.55 and λ_o = 6328Å

Experimental points are for gold films.

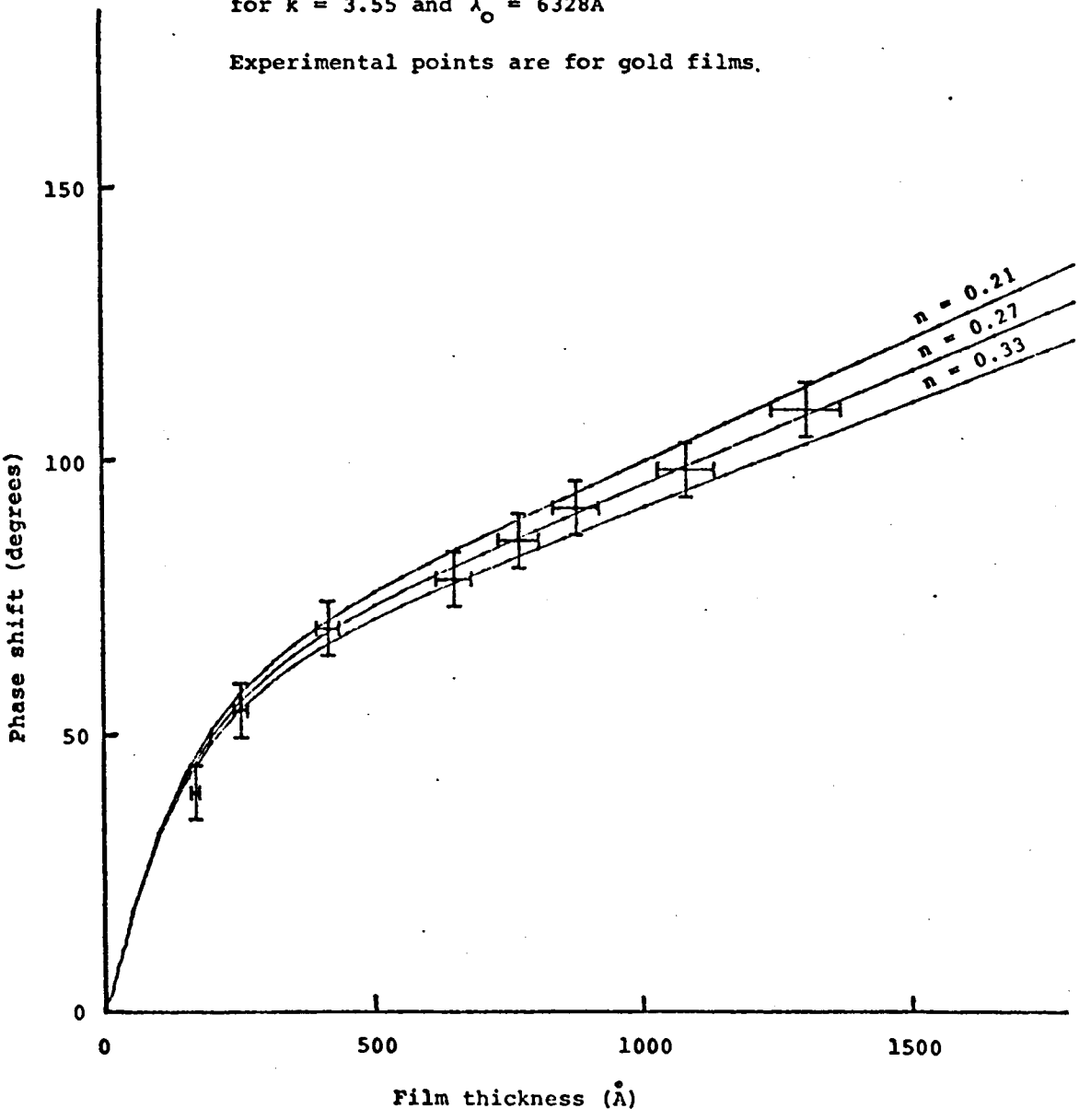

This iterative procedure is illustrated graphically in Figures 13 to 16 for λ_o = 6328Å, and Figures 15 and 16 are plotted using the final values of n and k determined from this procedure. Similarly, Figures 17 and 18 are plotted for λ_o = 5145Å, using the final values of n and k, and Figures 19 and 20 are plotted for λ_o = 4880Å, also using the final values of n and k.

Figure 17

OPTICAL DENSITY VS. THICKNESS
for n = 0.75 and λ_o = 5145Å

Experimental points
are for gold films.

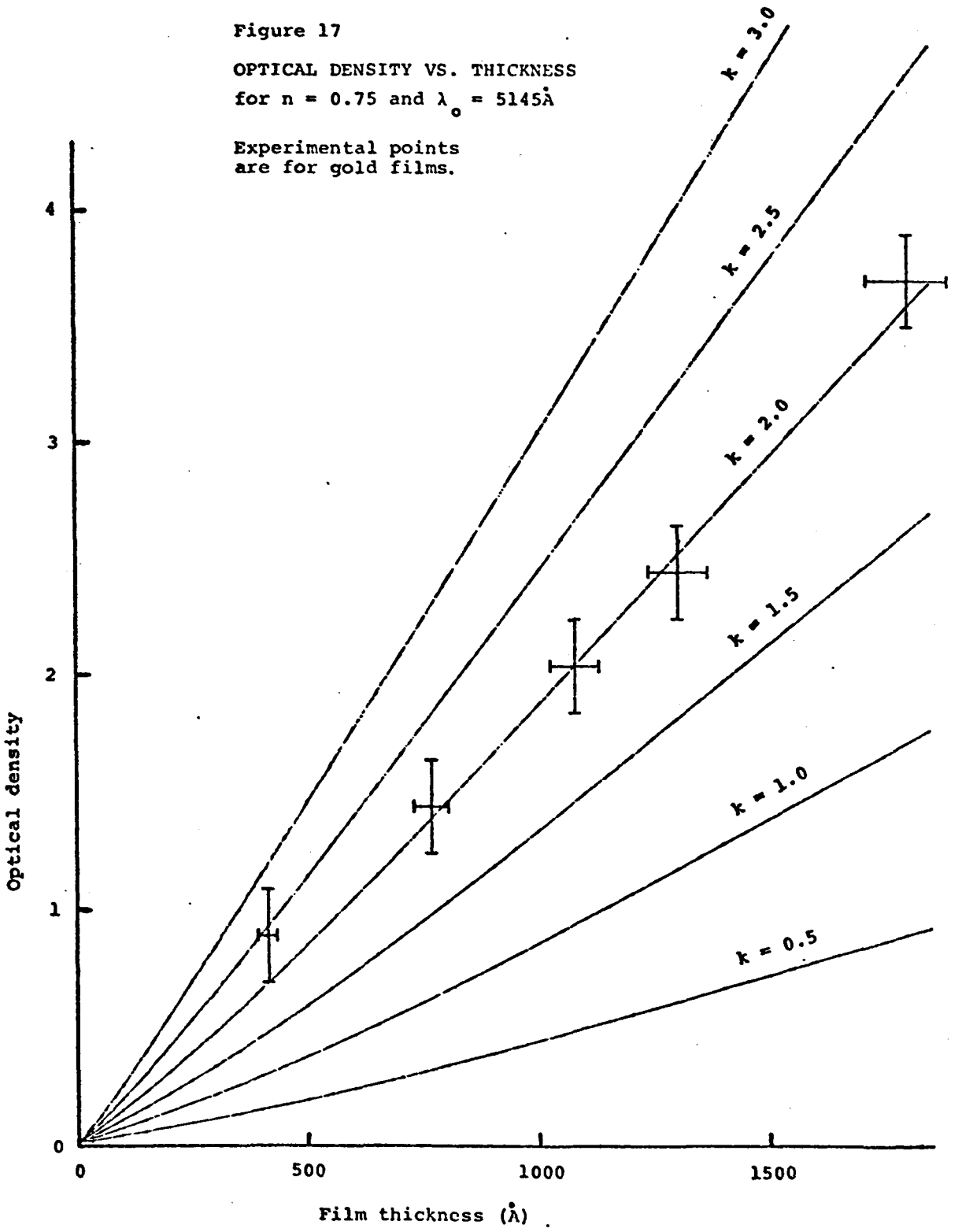

Figure 18

PHASE SHIFT VS. THICKNESS
for k = 2.0 and λ_o = 5145Å

Experimental points are for gold films.

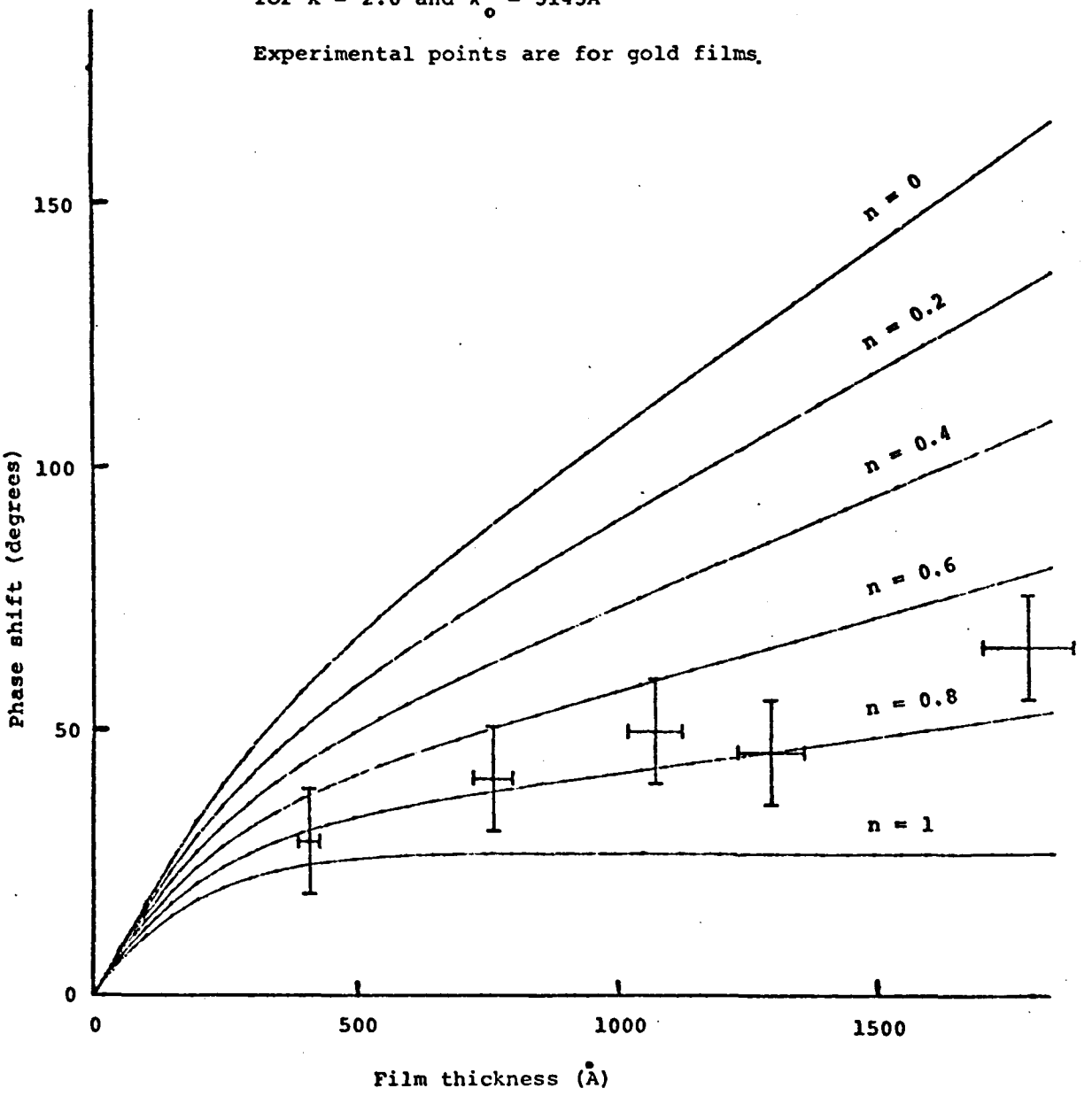

Figure 19

OPTICAL DENSITY VS. THICKNESS
for n = 1.15 and λ_o = 4880Å

Experimental points
are for gold films.

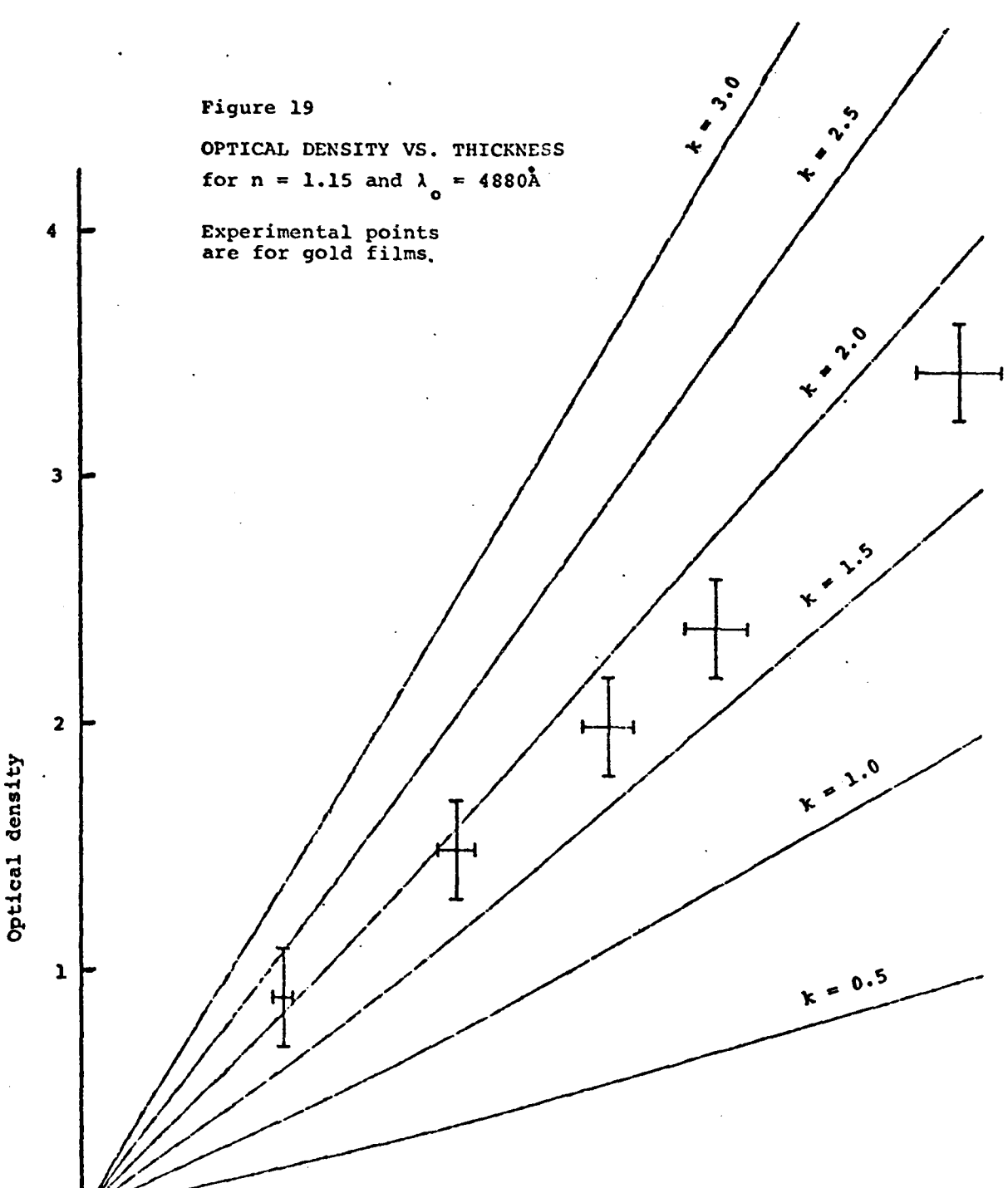

Figure 20

PHASE SHIFT VS. THICKNESS
for k = 1.8 and λ_o = 4880Å

Experimental points are for gold films.

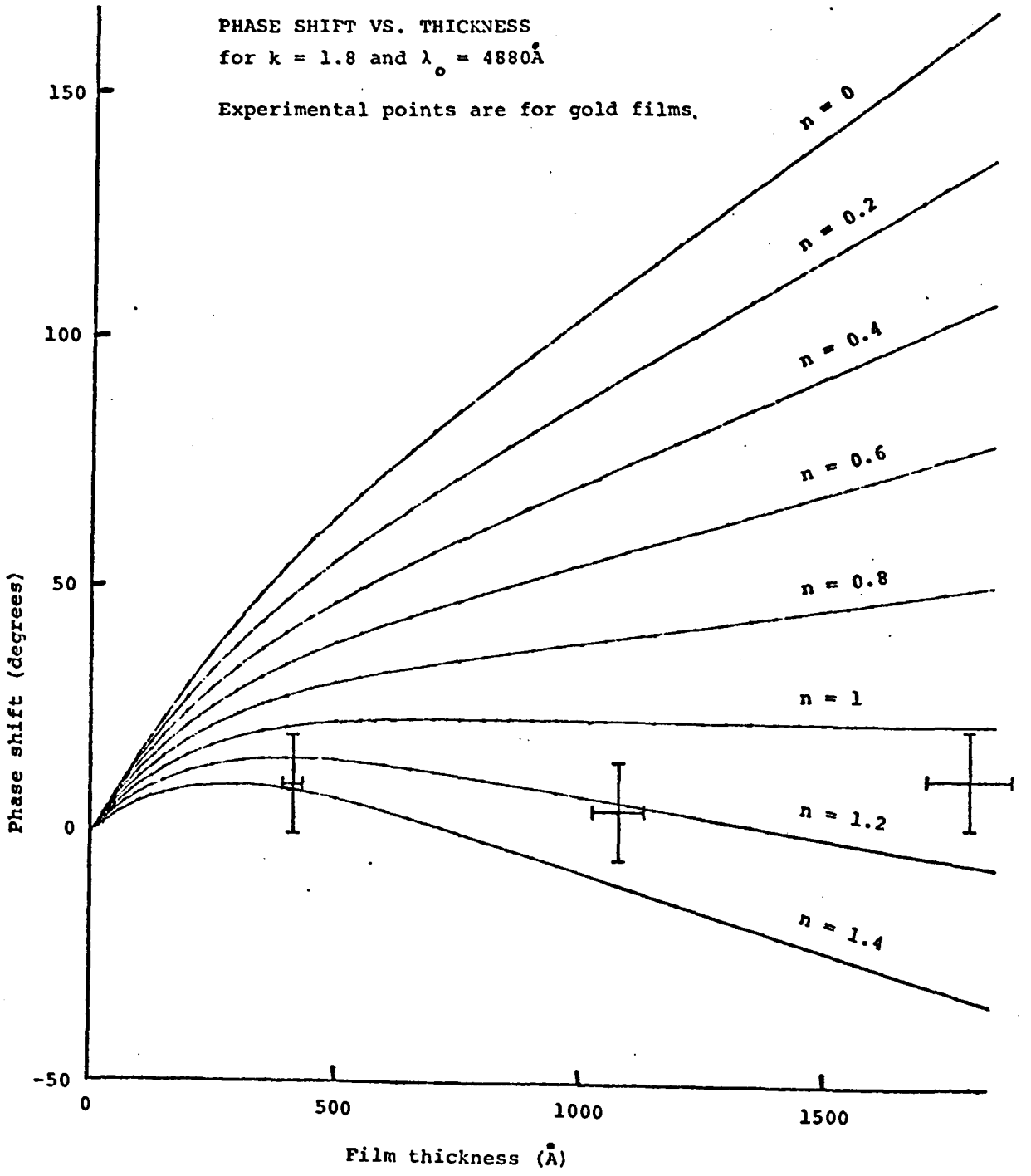

To indicate the rapidity of convergence of the iterative procedure, the optical density is plotted against d in Figure 21 for various values of n, at a particular value of k. Note the insensitivity with respect to the choice of n. Also, the phase shift ψ is plotted as a function of d in Figure 22 for various values of k, at a particular value of n. k is associated with absorption, thus largely determines the optical density. Correlatively, n is related to the wavelength of light inside the material, hence largely determines ψ.

Figure 21

OPTICAL DENSITY VS. THICKNESS
for $k = 3.55$ and $\lambda_o = 6328\text{Å}$.

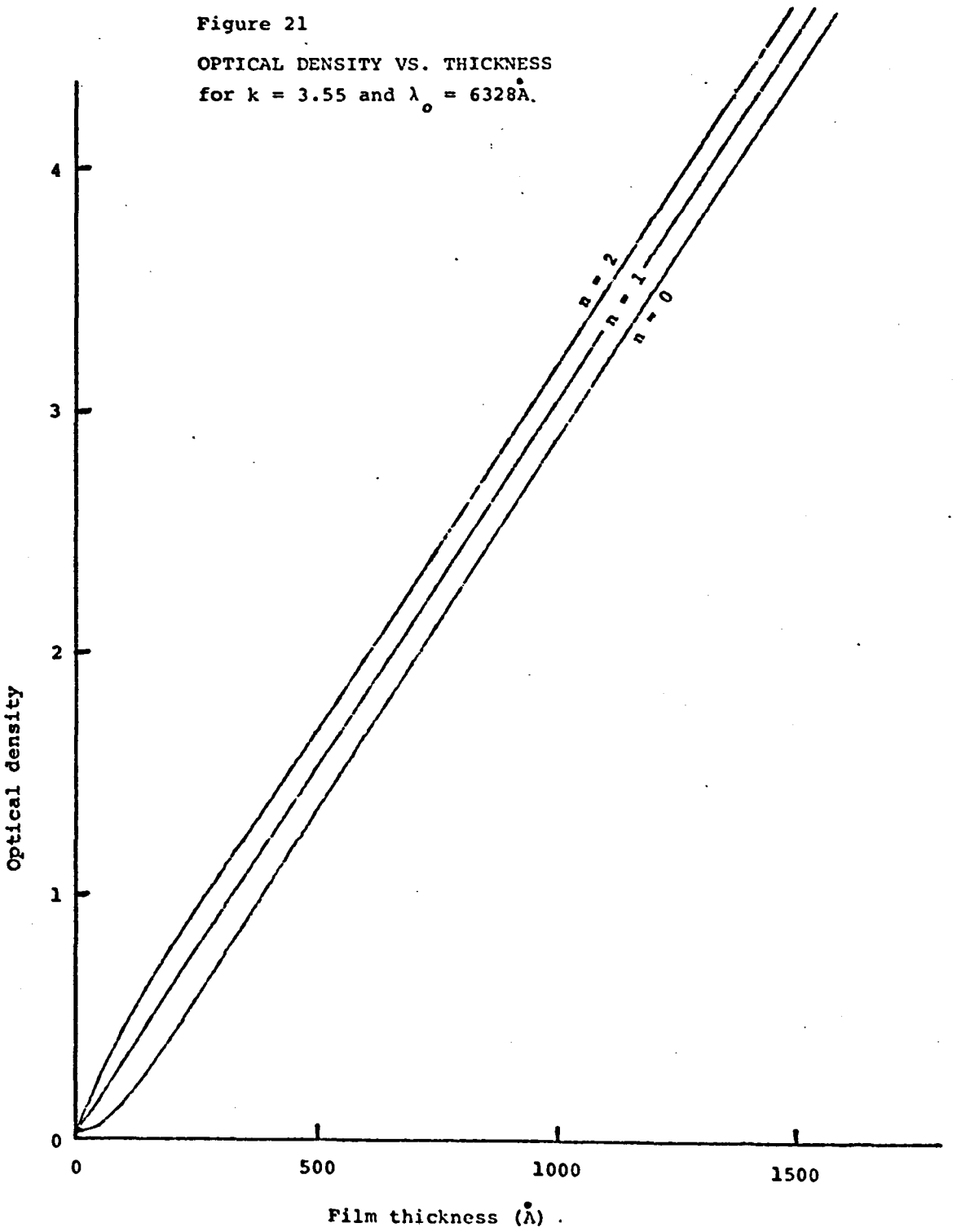

Figure 22

PHASE SHIFT VS. THICKNESS
for n = 0.27 and λ_o = 6328Å.

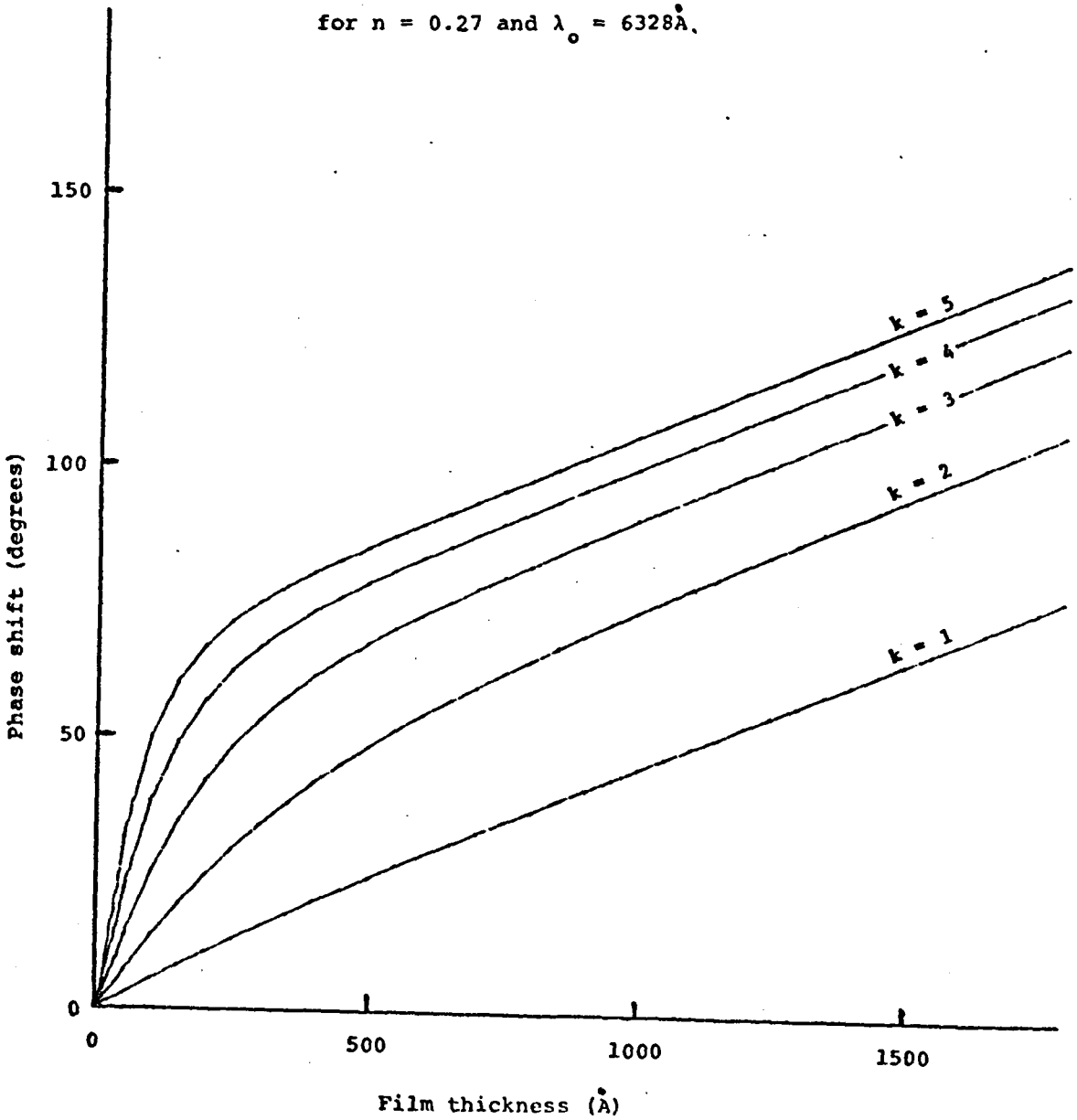

Our final values of n and k, determined using the general theory, are listed in Table III.

Table III. n and k for Gold, Determined from the General Theory. These values are influenced by surface effects. The "correct" values of n and k are listed in Table II.

λ_o (Å)	n	k
6328	0.27 ± 0.06	3.55 ± 0.15
5145	0.75 ± 0.08	2.00 ± 0.15
4880	1.15 ± 0.1	1.80 ± 0.15

A tentative assessment of surface effects is now possible. In Figures 14 or 16, for example, it is clear that an addition of approximately 5° to all of the phase shift measurements at $\lambda_o = 6328\text{Å}$ would bring the experimental points into agreement with the curve for n = 0.20, which is the "correct" value of n determined by the technique which eliminated surface effects by using only the thickness dependences of the measurements in the thick-film limit. It is thus possible that the sum of the phase shifts at the surfaces was approximately 5° greater than that which would be consistent with the theory of section 2-2. Similar deviations are noted at $\lambda_o = 5145\text{Å}$ and at $\lambda_o = 4880\text{Å}$. At $\lambda_o = 6328\text{Å}$, a noticeable

difference is present in the values of k determined by the two methods. A definite statement on the magnitude of the surface contributions is not justified at this point, because the observed deviations are comparable to the uncertainties in the measurements.

4-4 Discussion of the Results

The results of Johnson and Christy (1972), as well as those of Schulz (1954), and Schulz and Tangherlini (1954), are compared with our values (from Table II) of n and k for gold in Figures 23 and 24. Our results are in agreement, within experimental error. The large uncertainty in our value for n at λ_o = 4880Å arises from our having used only two points corresponding to the two thickest films in the plot of phase shift versus thickness.

Hunderi (1972) and Thèye (1970) have measured ε_1 and ε_2 for gold; Pells and Shiga (1969) have measured ε_2. The values of ε_1 and ε_2, calculated using our values of n and k in equations (15) and (16) are in agreement, within our experimental uncertainty, with the above authors' values. Johnson and Christy's results differ substantially from Thèye's at photon energies of 3eV to 5eV (that is, at wavelengths shorter than 4000Å), and Johnson and Christy believe that this discrepancy arises because Thèye's films were too thin ($d \approx 150$Å) to give bulk values. In the wavelength range 4880Å to 6328Å, the results obtained by all of the above authors agree with ours, within our experimental error, although they do not all agree with each other. For example, Pells and Shiga's values of ε_2 for gold are greater than Johnson and Christy's.

Figure 23.

n vs. λ_o for gold.

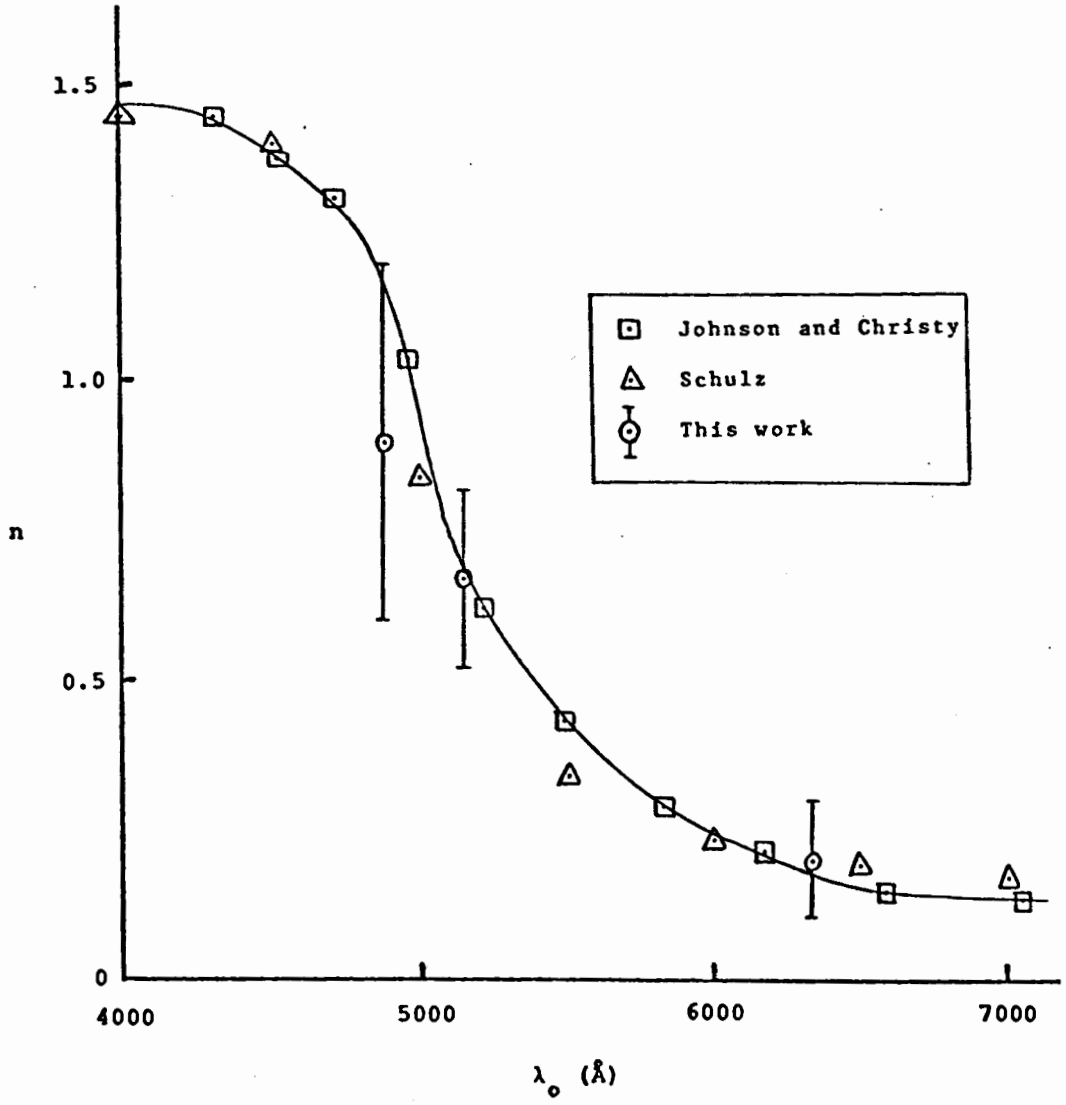

Figure 24.

k vs. λ_o for gold.

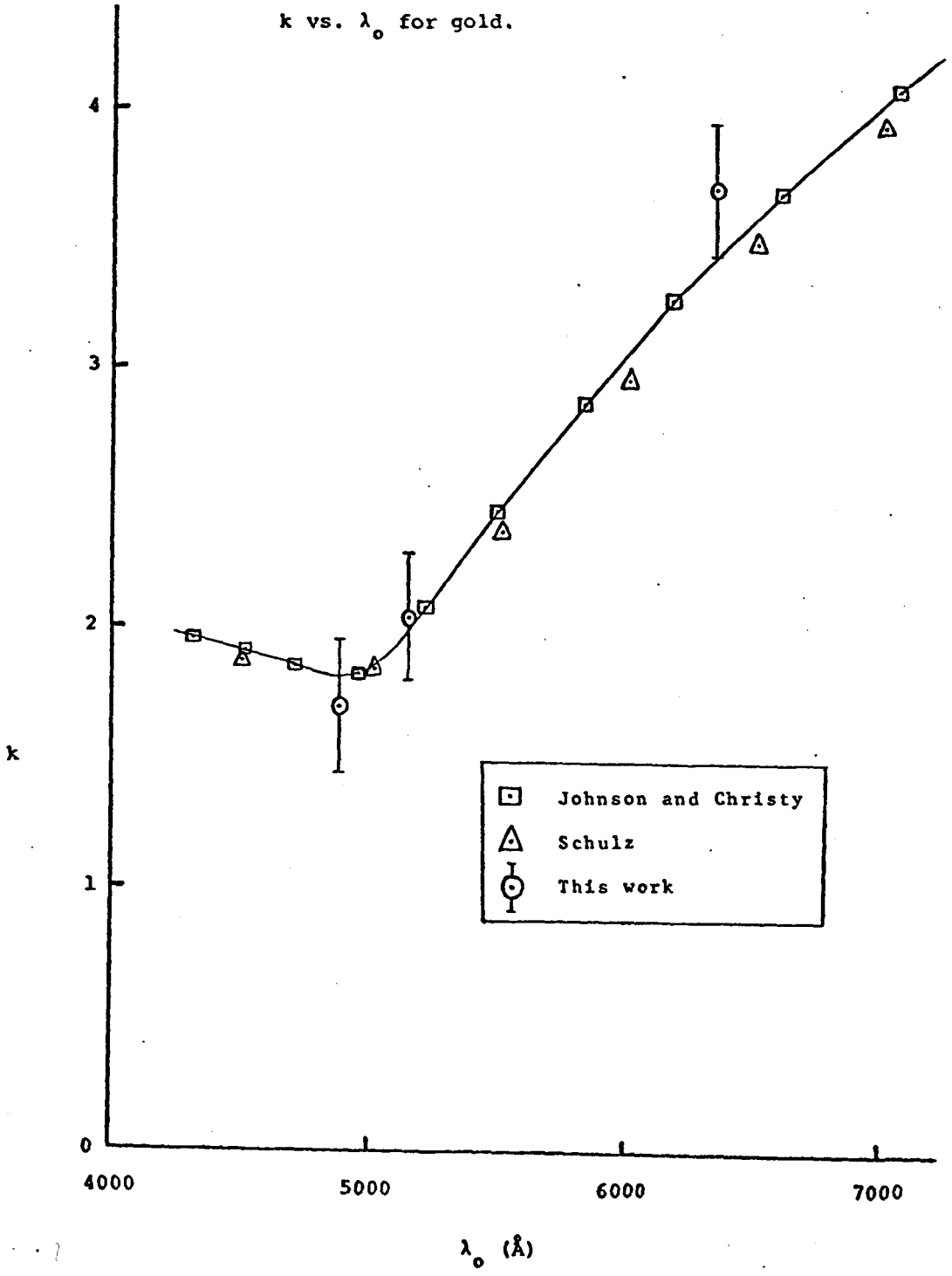

4-5 Suggestions for Improving the Accuracy of the Results

The accuracy of values of n and k obtained using our method could be improved, possibly to an accuracy comparable to that obtained by Johnson and Christy (1972) who state that their method, using reflection and transmission measurements on films less than 500Å thick, yields results for n and k accurate to ±0.02.

Errors in phase shift measurements could be reduced by enclosing the interferometer in an evacuated chamber, and the accuracy of the transmissivity measurements could be increased by using better calibration filters. A difficulty with using neutral density filters is that multiple reflections occur when filters are employed in a series; a superior calibration technique might be to use a constant-length absorption cell containing a solution of variable concentration.

The accuracy of the thickness measurements could be improved by adopting any of the more accurate (and more time-consuming) methods (Heavens, 1965, Chapter 5). One fairly easy way of making more accurate thickness measurements could be to have a rotating shutter between the source and substrate during evaporation, producing (simultaneously) a series of films of accurately-known relative thickness. The thickness of the thickest film could then be measured using the techniques described in section 3-3, and the thicknesses of the thinner films would then be known. (The thick film need not be used in the transmissivity or phase shift measurements.) In

addition, the thickness of the thinnest film could be measured using the x-ray technique mentioned at the end of section 3-3. This would provide accurate thickness measurements at both extremes of the range, and would permit accurate interpolation to intermediate thicknesses.

CHAPTER 5

CONCLUDING REMARKS

5-1 Comments and Conclusions -- Evaluation of the Technique

This thesis has demonstrated the feasibility of determining the optical constants of metals using a transmission technique in which both the transmissivity and the phase shift of the transmitted light are measured. The main advantage of this transmission method, compared to reflection methods, is that it provides direct information on the bulk properties of the material. Surface effects can be eliminated by using samples of sufficient thickness that multiple reflections may be neglected. In this thick-film limit, when one sample is compared with another of different thickness, assuming the surfaces of the two samples have identical properties, the difference in transmissivity or the difference in the phase change on transmission is due only to the difference in distance of bulk material through which the light has passed.

Reflection measurements, on the other hand, can be performed using a single sample, whereas the transmission technique described in this thesis has the disadvantage that it requires the fabrication of several samples of different thickness. This is not a serious detriment, however, since a suitable set of samples can be produced in a single evaporation run, and the only disadvantage is in the time and effort

required for the additional measurements. In addition, the preparation and storage of samples is not as critical in our case as it is for reflection measurements, because of the relative insensitivity of transmission measurements to surface contamination.

At present, our technique enables n to be determined, at a particular wavelength, to roughly the same absolute accuracy (±0.1 at λ_o = 6328Å) regardless of the magnitude of n. Thus the percentage uncertainty in the value of n is greater for materials with small n. Silver, for example, has a relatively small value of n ($\approx$ 0.05) for λ_o in the visible portion of the spectrum (Johnson and Christy, 1972; Shklyarevskii and Korneeva, 1971; Schulz and Tangherlini, 1954). Consequently, the wavelength of light is very long inside a silver film, and the phase change in traversing the film (excluding the phase changes at the surfaces) is very small. Our technique in its present form is thus not suitable for measuring n for silver, although an approximate value has been obtained.

Similar limitations on the accuracy of n are also present in Schulz's technique, which uses measurements of reflectivities on the metal side and on the substrate side of the sample (Schulz, 1954, p. 367); although the estimated error in n is somewhat smaller for smaller n, the percentage error still increases as n decreases. Johnson and Christy's uncertainty in the value of n is nearly constant (±0.02); consequently

their results also exhibit a large percentage error if n is small. (Johnson and Christy's uncertainty in the value of n for silver is ±40% for λ_o in the visible.)

We now turn our attention to the accuracy of the values of k determined using the transmission technique. Note that our value of k for gold at $\lambda_o = 6328\text{Å}$ appears somewhat greater than Johnson and Christy's value, with the deviation just within the error range. It would be desirable to improve the accuracy of our transmissivity measurements (perhaps utilizing the suggestions in section 4-5) to ascertain whether the value of k determined from transmission measurements differs from the the value of k determined by means of an experiment that includes reflection measurements.

The region of the n-k plane in which our technique is least accurate is the domain of small n and large k. This happens to be the domain of high reflectivities, since, from equations (38) and (60), the normal-incidence reflectivity for a single air-metal interface is

$$R = \left| \frac{1-\hat{n}}{1+\hat{n}} \right|^2 = \frac{(1-n)^2+k^2}{(1+n)^2+k^2} \quad .$$

Thus for small n and/or large k, the reflectivity approaches unity. This range of values is encountered, for example, in the case of silver, which has both a large value of k (≈ 4.2 at $\lambda_o = 6328\text{Å}$) and a small value of n. However, one of these conditions without the other enables our technique to be used. For example, a strongly-absorbing material with a

reasonably large value of n can be studied because the phase change on transmission is measurable for thin films. Also, a weakly-absorbing material with a small value of n can be studied, since thicker films can be used to facilitate phase shift measurements.

With the anticipated improvements to achieve an ultimate accuracy, the transmission technique should have essentially unlimited applicability. The technique should be usable for silver, and since silver is the "worst case" (having both small n and large k), the technique should be suitable for any material. No material known to the author satisfies both $n < n_{silver}$ and $k > k_{silver}$ in the visible portion of the spectrum. (Aluminum has a larger value of k than silver, but the value of n is also greater for aluminum than for silver.)

5-2 Suggestions for Further Study

(a) Improvements in the accuracy capabilities of the technique, along the lines suggested in section 4-5, would lead naturally into several further experiments. For example, despite the large amount of work performed in the past, discrepancies in the reported values of the optical constants of metals still exist among different authors describing recent work. Accurate measurements would not only resolve these discrepancies but would also provide accurate values that could be compared to sophisticated calculations of the optical constants (Johnson and Christy, 1972, p. 4370).

(b) If the technique were capable of providing more accurate values, it would also enable a quantitative study of surface effects to be performed. A detailed comparison of the results obtained in the thick film limit with those obtained using the general theory could then be carried out, and discrepancies between the two sets of values would be a measure of the surface effects.

(c) Our phase shift measurements were performed using suspended films. Films on substrates could also be used, provided that the variations in thickness of the substrates are "mapped" in advance. For example, a cleaved piece of mica could be studied with the interferometer to find the cleavage steps, which would show up as steps in the measured phase shift. A film could then be deposited on the mica, and the phase shift for the film could be measured. This

procedure might be suitable for a material which is so strongly-absorbing that a film of appropriate thickness for phase shift measurements would be too thin, hence too fragile, to suspend over an aperture of reasonable size. Another possible motivation for using films on substrates is that one could, in an application similar to that proposed in suggestion (b), perform a quantitative evaluation of deviations from the bulk values of the optical constants near the surfaces of samples adjacent to various substrates.

(d) Highly reactive materials cannot be conveniently studied by reflection methods because of surface oxidation problems. The optical constants of such materials (e.g. thallium, which is also toxic) could be measured using our transmission technique by making "sandwiches" with various thicknesses of the material to be studied between layers of an inert protective material (e.g. carbon).

(e) It would be interesting to observe the variations in the optical constants of some material (e.g. cesium, with $\lambda_p \approx 4400\text{Å}$) while tuning through its plasma frequency with a dye laser. This could be done with our technique; the electro-optic modulator could be made broad-band by applying a d.c. voltage bias rather than using optical biasing in the form of the quarter-wave plate.

LIST OF REFERENCES

Abelès, F., "Optical Properties of Metallic Films", in Physics of Thin Films, Volume 6, edited by G. Hass and R. Thun, Academic Press, New York, 1971.

Born, M., and Wolf, E., Principles of Optics, 3rd (revised) edition, Pergamon, Oxford, 1965.

Brattain, W.H., and Briggs, H.B., The Optical Constants of Germanium in the Infra-red and Visible, Physical Review 75, 1705 (1949).

Croce, P., Devant, G., Sere, M.G., and Verhaeghe, M.F., Thin Film Surface Studies by X-Ray Reflection, Surface Science 22, 173 (1970).

Croce, P., Gandais, M., et Murraud, A., Étude sur la structure de couches minces d'or et d'indium, Revue d'Optique 40, 555 (1964).

Françon, M., Optical Interferometry, Academic Press, New York, 1966.

Garbuny, M., Optical Physics, Academic Press, New York, 1965.

Givens, M.P., "Optical Properties of Metals", in Solid State Physics, Volume 6, edited by F. Seitz and D. Turnbull, Academic Press, New York, 1958.

Haysman, P.J., and Lenham, A.P., Transmittance Method to Determine the Optical Constants of a Single Specimen, Journal of the Optical Society of America 62, 333 (1972).

Heavens, O.S., "Measurement of Optical Constants of Thin Films", in Physics of Thin Films, Volume 2, edited by

G. Hass and R. Thun, Academic Press, New York, 1964.

Heavens, O.S., Optical Properties of Thin Solid Films, Dover, New York, 1965.

Heavens, O.S., Thin Film Physics, Methuen, London, 1970.

Hunderi, O., New Method for Accurate Determination of Optical Constants, Applied Optics 11, 1572 (1972).

Jackson, J.D., Classical Electrodynamics, Wiley, New York, 1962.

Johnson, P.B., and Christy, R.W., Optical Constants of the Noble Metals, Physical Review B 6, 4370 (1972).

Kiessig, H., Interferenz von Röntgenstrahlen an dünnen Schichten, Annalen der Physik [5] 10, 769 (1931).

Klein, M.V., Optics, Wiley, New York, 1970.

Mozzi, R.L., and Guentert, O.J., Adaptation of an X-Ray Diffractometer for Thin Film Studies by Total Reflection of X-Rays, The Review of Scientific Instruments 35, 75 (1964).

Nestell, J.E., and Christy, R.W., Derivation of Optical Constants of Metals from Thin-film Measurements at Oblique Incidence, Applied Optics 11, 643 (1972).

Parratt, L.G. Surface Studies of Solids by Total Reflection of X-rays, Physical Review 95, 359 (1954).

Pells, G.P., and Shiga, M., The optical properties of copper and gold as a function of temperature, Journal of Physics C 2, 1835 (1969).

Purcell, E.M., Electricity and Magnetism, Berkeley Physics Course - Volume 2, McGraw-Hill, New York, 1965.

Schulz, L.G., The Optical Constants of Silver, Gold, Copper, and Aluminum -- I: The Absorption Coefficient k, Journal of the Optical Society of America 44, 357 (1954). Note that Schulz calls k the absorption coefficient, whereas we call k the extinction coefficient and α the absorption coefficient -- see equation (20).

Schulz, L.G., and Tangherlini, F.R., Optical Constants of Silver, Gold, Copper, and Aluminum -- II: The Index of Refraction n, Journal of the Optical Society of America 44, 362 (1954).

Schulz, L.G., The Experimental Study of the Optical Properties of Metals and the Relation of the Results to the Drude Free Electron Theory, Quarterly Supplement to the Philosophical Magazine 6, 102 (1957).

Shklyarevskii, I.N., and Korneeva, T.I., Optical Constants of Silver Thin Films, Optics and Spectroscopy 31, 144 (1971).

Thèye, M.-L., Investigation of the Optical Properties of Au by means of Thin Semitransparent Films, Physical Review B 2, 3060 (1970).

Wainfan, N., Scott, N.J., and Parratt, L.G., Density Measurements of Some Thin Copper Films, Journal of Applied Physics 30, 1604 (1959).